NASA TECHNICAL NOTE

NASA TN D-4394

NASA TN D-4394

AN INVESTIGATION OF LEAKAGE OF LARGE-DIAMETER O-RING SEALS ON SPACECRAFT AIR-LOCK HATCHES

by Otto F. Trout, Jr.

Langley Research Center
Langley Station, Hampton, Va.

NATIONAL AERONAUTICS AND SPACE ADMINISTRATION • WASHINGTON, D. C. • MARCH 1968

AN INVESTIGATION OF LEAKAGE OF LARGE-DIAMETER O-RING SEALS ON SPACECRAFT AIR-LOCK HATCHES

By Otto F. Trout, Jr.

Langley Research Center
Langley Station, Hampton, Va.

NATIONAL AERONAUTICS AND SPACE ADMINISTRATION

For sale by the Clearinghouse for Federal Scientific and Technical Information
Springfield, Virginia 22151 – CFSTI price $3.00

AN INVESTIGATION OF LEAKAGE OF LARGE-DIAMETER O-RING SEALS ON SPACECRAFT AIR-LOCK HATCHES

By Otto F. Trout, Jr.
Langley Research Center

SUMMARY

An investigation has been conducted to determine the leakage of large-diameter O-ring seals for operable hatch doors and static joints with a vacuum of 1.0×10^{-6} torr (1.33×10^{-2} N/m2) on one side and atmospheric pressure on the other. The measuring techniques employed made it possible to determine the leakage of any hatch component of an air-lock system. Tests of O-ring seals 28 to 30 inches (0.71 to 0.76 meter) in diameter have indicated that helium leakages of less than 1.0×10^{-5} cc/sec (STP) are attainable with butyl, viton, and neoprene elastomers for operable hatch doors and static seals. Silicone elastomeric O-rings allowed considerably greater leakages. The results indicate that the leakage of O-ring seals is sufficiently low for atmospheric containment on manned spacecraft under the conditions of this investigation.

INTRODUCTION

Feasibility studies by the Langley Research Center on manned orbital vehicles and interplanetary spacecraft have shown a lack of quantitative engineering data on the performance of seals and air-lock systems under high-vacuum conditions. In addition, these studies have shown the need for determining seal problem areas, establishing a better understanding of seal theory and mechanisms, establishing attainable design leakage values, and experimentally verifying pertinent design factors necessary to achieve reliable sealing of large lightweight structures.

The main areas to be sealed aboard a manned spacecraft are the life-support compartment, the structural shell, air locks, docking ports, hydraulic, pneumatic, and electrical connectors, and vent ports. The results of research into suitable seals for each of these areas for manned spacecraft (ref. 1) have indicated that a knowledge of the technology must include the structural loading for reliable sealing, the choice of suitable seal materials, the environmental effects on the seal, and attainable leakage values measured under actual operating conditions.

References 1 and 2 indicate that structural loading and choice of seal materials are strongly interrelated. Elastomeric seal materials are sufficiently resilient to maintain at least the minimum seating stress required for effective sealing of large lightweight structures without imposing excessive loads. The effects on seal materials of exposure to high vacuum for long periods of time, temperature extremes, and electromagnetic and particulate radiation have been studied by a number of researchers and are summarized in reference 3.

Leakage rates calculated from the permeation rates of gases through elastomers (refs. 3 and 4) would be acceptable for atmospheric containment on manned spacecraft. However, because of unknown joint and seal defects, seal leakage cannot be accurately predicted. The present research program was undertaken, therefore, to obtain actual measurements on lightweight spacecraft structures.

A vacuum chamber was constructed which was capable of testing full-size spacecraft air-lock systems and component parts. The vacuum test chamber will be described briefly in the present report.

As part of a continuing program, a model of a spacecraft air lock was constructed and leakage tests were made on the various seal areas under high-vacuum conditions. Leakage was measured with four different elastomeric O-ring materials: butyl, neoprene, viton, and silicone. In order to investigate the effects of the direction of loading on the leakage of an operable hatch, measurements were made with the hatch forced toward the closed position by pressure and with the hatch forced toward the open position by pressure. In addition, the reliability of the hatch seals was investigated by measuring leakage before and after 50 cycles of operation. The leakage of large O-rings in two different types of grooves in the hatch was measured. In addition, O-ring leakage was measured for static bolted and clamped joints.

The results of this investigation, as well as a description of the test equipment, instrumentation, and methods for determining leakage, are described herein.

EQUIPMENT

Air-Lock Test Model

The air lock, shown in figure 1, was constructed of 2014-T6 aluminum alloy. It had an overall length of 91 inches (2.31 meters) including the hatch doors at each end (doors closed). The cylindrical section of the air lock had an outside diameter of 31.5 inches (0.80 meter) excluding flanges and a minimum inside diameter of 28 inches (0.71 meter) at the hatch seating frame. The cylindrical section was divided into five individual segments. Joints 1 and 2 were fastened with 36 bolts and each was sealed with a single

elastomeric O-ring. Joint 3 was fastened with 16 toggle clamps and sealed with two elastomeric O-rings in series. A flange of 54-inch (1.37-meter) diameter was used to mount the air-lock model on the vacuum test facility.

Hatch doors 1 and 2 were identical and were constructed of aluminum alloy sheet 0.062 inch (1.6 mm) thick bonded to an aluminum honeycomb core and to an aluminum alloy outer rim and center spindle. A cam-actuated latching mechanism which can be controlled by handles on either side of the hatch door, as illustrated in figure 2, provides the necessary seating forces on the seal. The latch mechanism was designed to withstand a differential pressure across the hatch of 1 atmosphere with a design safety factor of 4.

O-Ring Seals and Seal Areas

The hatch seals, as shown in figure 2, were elastomeric O-rings having a nominal cross-section diameter of 0.275 inch (7.0 mm). Four different elastomeric materials were tested: butyl, neoprene, viton, and silicone. Seating surfaces for the O-rings were machined to a finish of 32 microinches (8.1×10^{-4} mm) or better. Figure 3 is a diagram of the cross section of the hatch seated in the hatch frame. An undercut trapezoidal groove (seal groove 1) is used to contain the O-ring for the face seal. The dimensions for this groove are shown in detail B of figure 4. With an O-ring of 0.275-inch (7.0-mm) nominal diameter, a 0.040-inch (1.0-mm) compression of the O-ring cross-sectional diameter results. This is standard dimensional practice for O-rings in undercut grooves (ref. 5).

Figure 5 presents a diagram of the actuator shaft for the latch mechanism and the accompanying shaft seals in the center of the hatch. The shaft is sealed with O-rings having a cross-section diameter of 0.139 inch (3.5 mm) seated in grooves as detailed in figure 5 and lubricated with a high-vacuum silicone grease.

Figure 6 is a typical diagram of static joints 1 and 2. The cylindrical segments are bolted together and sealed with a single elastomeric O-ring. The O-ring has a cross-section diameter of 0.275 inch (7.0 mm) and is seated in a groove having the dimensions shown in figure 7. The cross-section diameter is compressed 0.069 inch (1.7 mm) when the O-ring is seated.

Figure 8 presents a diagram of joint 3, which was sealed with two O-rings, each having a cross-section diameter of 0.275 inch (7.0 mm), seated in grooves having the dimensions of detail A, figure 4. The joint was fastened with 16 toggle clamps equally spaced on the periphery.

The O-rings used in the hatch and static seals were made from commercially extruded elastomers. They were cut to length and the ends were vulcanized together to

form the required diameter. The O-ring for the actuator shaft through the center of the hatch was a commercially molded seal. The surfaces of O-rings formed from extruded stock were considerably rougher than those of molded O-rings. The cross-section diameter of the O-rings varied along the length of the extruded stock and among the different elastomers, as shown in table I.

Before testing, each of the O-rings was washed with alcohol and the grooves were cleaned with acetone. Since the permeability of elastomers can be decreased by lubricants, the O-rings were used dry in all tests except for the rotating shaft seal through the center of the hatch.

Test Facility

The vacuum test chamber, shown in figure 9, consists of a tank 8 feet (2.44 m) in diameter by approximately 8 feet (2.44 m) long, with a volume of approximately 544 cu ft (15.4 m^3). It is attached to a 32-inch-diameter (0.81-m) oil diffusion pump with a capacity of 1840 cu ft (52 m^3) per second. Incorporated in the top of the diffusion-pump system is a water-cooled baffle, above which is a liquid-nitrogen baffle. A pneumatically operated high-vacuum valve 32 inches (0.81 m) in diameter is used to isolate the test chamber from the pumping system. For roughing, a rotary piston pump with a capacity of 500 cu ft (14 m^3) per minute is used in connection with the diffusion pump (fig. 10). When the test chamber is isolated by the high-vacuum valve and the diffusion pump is not in use, vacuum is maintained on the diffusion pump by a rotary holding pump with a capacity of 15 cu ft (0.424 m^3) per minute.

Figure 11 is a photograph of the air-lock model mounted on the test chamber, with hatch 2 inside the vacuum test facility. The mounting plate contains a 48-inch (1.22-m) opening into the test section and a 52-inch (1.32-m) bolt circle for attachment of test models. The model is sealed to the test chamber with a single butyl O-ring compressed 25 percent of its cross-section diameter in a rectangular groove.

The vacuum system is capable of pumping the test chamber from atmospheric pressure to 1×10^{-6} torr (133×10^{-6} N/m^2) in a period of 2 hours, and to an ultimate pressure of 1×10^{-7} torr (133×10^{-7} N/m^2) when the chamber is closed without a test model.

Instrumentation

Instrumentation for the test section, as illustrated in figure 11, consists of a Bourdon absolute-pressure gage for measuring pressures from 1 to 800 mm Hg (133 to 107 000 N/m^2), a thermocouple-type conductivity gage for measuring pressures of 5 to 1000 microns (0.133 to 133 N/m^2), and an ionization gage installed in the side of the vacuum test chamber to measure pressures of 1×10^{-4} to 1×10^{-8} torr (133×10^{-6} to

133×10^{-8} N/m^2), with direct readout and recording on a strip chart. An additional ionization gage, not shown in the photograph, was also used for direct readout and calibration.

The controls and accompanying indicators for the vacuum pumping system are shown in figure 11. An additional thermocouple conductivity gage is used to measure the absolute pressure in the line between the diffusion pump and the mechanical pump.

Figure 12 is a diagram of the helium mass-spectrometer leak detector used to determine leakage rates by continuously sampling the output of the diffusion pump from the line to the mechanical roughing pump. The leak detector is capable of detecting leaks of helium as small as 2×10^{-10} cc/sec; however, because of outgassing effects and dilution from other leakage sources, the sensitivity of the system used in the present tests was reduced to about 1×10^{-7} cc/sec.

Two calibrated leakage sources of the porous-plug type, shown in figure 13, were used to bleed known leakages of helium into the test chamber to calibrate the helium mass spectrometer. One calibrated leakage source shown here had a range of 6.6×10^{-2} to 5.29×10^{-3} cc/sec (STP) while the other source had a range of 7.1×10^{-4} to 1.0×10^{-6} cc/sec (STP).

TESTS AND PROCEDURES

Tests

All tests were conducted with the air-lock model mounted on the vacuum test chamber as shown in figure 11. Separate leakage rates were determined for the whole exposed end of the test model, each hatch door with four different seal materials, and each externally exposed static joint. This was accomplished by encapsulating the involved area of the model with a polyethylene bag. Helium was pumped into the encapsulated bag and the leakage rate was determined by methods described in the next section. A summary of these tests and the resulting leak rates is presented in table II.

For tests 1 to 12 and 21 to 23, hatch 1 was closed and hatch 2 was left open so that the interior of the air lock was evacuated, while for tests 13 to 20, hatch 2 was closed and hatch 1 was left open, exposing the interior of the air lock to atmospheric pressure and the outside of hatch 2 to vacuum. During leakage measurements, equilibrium vacuum conditions between 9×10^{-7} and 2×10^{-6} torr (1200×10^{-7} and 267×10^{-6} N/m^2) were maintained.

Leakage measurements were made first for the entire end of the air lock. During these tests, butyl seals were in all three grooves of hatch 1 and in static joints 1, 2, and 3. The encapsulation of the exposed end of the air lock for these tests is shown in figure 13.

Successive leakage measurements were made with single O-ring seals of butyl, neoprene, viton, and silicone in seal groove 1 of hatch 1. One test was also made to determine the leakage of a single butyl seal in groove 2 of hatch 1. During the tests, hatch 1 was opened and sealed 50 successive times and the leakage was measured after 1 cycle and after 50 cycles.

Next, leakage measurements were made on hatch 2 with single O-ring seals of butyl, neoprene, viton, and silicone in groove 1. During these tests, hatch 1 was left open so that the interior of the air lock was at atmospheric pressure.

Finally, leakage measurements were made with butyl O-rings on static joints 1, 2, and 3 separately, with the inside of the air lock evacuated. An attempt was made to measure the leakage past the seals on the actuation shaft of hatch 1 (fig. 5); however, leakage was below the detectable range of the instrumentation.

Leakage-Measuring Techniques

When leaks into a large-volume container are so small that they cannot be measured by pressure changes over a finite period of time and/or when outgassing and other unknown leakage sources make measurement difficult, specialized techniques are required. One measurement technique useful in high-vacuum work is to isolate the particular leakage area, flood the area with helium, and measure leakage of helium into the vacuum system.

Figure 13 shows the exposed end of the air lock encapsulated in a plastic bag so that helium can be injected into the isolated area and the overall seal leakage can be measured. In a similar manner, any specific seal area may be isolated and the leakage measured. Figure 10 is a diagram of the leakage-measuring system used in the present series of tests. A helium mass spectrometer (fig. 12) continuously withdraws and analyzes samples of the gas from the foreline of the diffusion pump which is continuously pumping on the test chamber and model. When the vacuum test chamber reaches a stable pressure level, the plastic bag isolating the leakage area to be measured is evacuated with a separate vacuum pump, and helium gas is injected into the encapsulated area. Helium passes through any leakage points into the interior of the test chamber, where it mixes with air leaking from other areas and with outgassing products from the interior of the chamber and air lock.

The partial pressure of helium in the mixture is measured by the mass spectrometer. After the measurement, helium is removed from the encapsulated area. The system is then calibrated against a known leakage of helium. This calibration is accomplished by injecting helium into the test chamber through a calibrated leak to mix with the air leakage and outgassing products, and again measuring the partial pressure of helium with the helium mass spectrometer. The calibrated leakage sources (fig. 13)

consist of an enclosed porous metal disk through which helium permeates at a rate determined by the differential pressure.

Accuracy and Sources of Error

The usefulness, limitations, and accuracy of this leakage measuring system can be described in terms of dilution ratio by the following simplified equation for steady-state conditions:

$$D = \frac{V_{He} + V_G + V_A + V_B}{V_{He}} = 1 + \frac{V_G + V_A + V_B}{V_{He}}$$

where

D dilution ratio, ratio of volume of total gases to volume of helium

V volume of gas per unit time entering chamber at standard conditions of temperature and pressure

and subscripts

He helium leakage through isolated area or calibrated leak

G outgassing products from interior of system

A air leakage from all sources other than isolated area

B air leakage through isolated area

Under steady-state conditions (denoted by subscript 1) the total leakage and outgassing of the vacuum system can be expressed by

$$V_1 = V_{G,1} + V_{A,1} + V_{B,1}$$

Although V_1 is not directly measurable, its stability can be determined and its value calculated approximately from the pumping speed and equilibrium pressure of the vacuum system.

During the measurement of leakage through an isolated area (subscript 2) the equation for dilution ratio reduces to

$$D_2 = \frac{V_{He,2} + V_{G,2} + V_{A,2}}{V_{He,2}} = 1 + \frac{V_{G,2} + V_{A,2}}{V_{He,2}}$$

During calibration against a calibrated leak (subscript 3) the equation becomes

$$D_3 = \frac{V_{He,3} + V_{G,3} + V_{A,3} + V_{B,3}}{V_{He,3}} = 1 + \frac{V_{G,3} + V_{A,3} + V_{B,3}}{V_{He,3}}$$

The term $V_{B,3}$ enters the equation because air can leak through the isolated area.

The accuracy and usefulness of the measuring system is greatest when the dilution ratios D_2 and D_3 are equal; in practice, this condition can only be approximated for the following reasons:

(a) $V_{G,2} + V_{A,2}$ must be kept nearly equal to $V_{G,3} + V_{A,3}$ during leakage measurement and calibration by maintaining stable outgassing and leakage conditions.

(b) The accuracy of the calibration decreases as $V_{B,3}$ approaches $V_{G,3} + V_{A,3}$.

(c) The accuracy decreases as $V_{He,2}$ approaches $V_{G,2} + V_{A,2}$ or $V_{He,3}$ approaches $V_{G,3} + V_{A,3}$.

Leakage measurements for dilution ratios between 2 and 100 000 are practical with this system under stable conditions, with decreasing accuracy at the two extremes. In the present investigation leakage measurements of 10^{-3} cc/sec to 10^{-7} cc/sec were made for a useful range of about 4 orders of magnitude, with calculated dilution ratios of 38 to 65 000.

The major sources of error in the use of this leakage measuring technique arise from differences in outgassing rates and changes in dilution ratio between calibration and measurements, and from instrumentation errors. Calibrations against known leakage sources are repeatable within ±5 percent under stable outgassing conditions. Maintenance of outgassing stability within 5 percent between calibration and measurement becomes impractical under operational conditions unless the chamber and air locks are continuously pumped for several days or the entire system is baked out. Baking requires temperatures which would change the basic characteristics of the elastomeric seal materials.

RESULTS

Leakage measurements were made for the entire exposed section of the air lock, each of the two hatches with four different seal materials, and each of the exposed static sealed joints. The results of these tests are given in table II and plotted as a function of time after the application of helium in figures 14 to 27. Leakage measurements were made at ambient room temperature, 72° to 76° F (23° to 25° C); however, they are reported at standard conditions of temperature and pressure since corrections are negligible.

Exposed End of Air Lock

Leakage measurements for the entire exposed section of the air lock are plotted as a function of time after application of helium in figure 14. Tests were conducted on three successive days without opening the hatch, to check repeatability and trends for application to subsequent tests. It was evident that some finite time was required for helium to permeate the seal material at an equilibrium rate and also for the gas mixtures within the test chamber to reach equilibrium after helium application. Figure 14 indicates that the leakage rate was increasing when tests 1 and 2 were terminated. Test 3, therefore, was continued for 30 hours. A maximum leakage of 5.2×10^{-5} cc/sec (not shown in fig. 14) was measured after about 3 hours and a slightly lower value after 30 hours. The results of these tests for atmospheric containment indicate that the leakage of helium through butyl seals would be extremely small aboard a manned space vehicle.

An interesting phenomenon was that after the test the hatch door could not be opened manually when the pressure was equalized across it because of the vacuum retained between the seals. For this reason seals in series are not suitable for hatches that are held closed by pressure, unless bleeds are provided.

Hatch 1

Figure 15 presents the leakage measurements for a single O-ring in groove 1 of hatch 1, for four different types of hatch seals: butyl, neoprene, viton, and silicone. The hatch was pressure-loaded toward the closed position. The maximum leakage for the butyl seal was 1.05×10^{-6} cc/sec; for the viton, 2.8×10^{-6} cc/sec; for the neoprene, 4.3×10^{-6} cc/sec; and for the silicone, 1.12×10^{-4} cc/sec. While the leakage rates of butyl, neoprene, and viton O-ring seals were of the same magnitude, leakage for the silicone was about 1 to 2 orders of magnitude greater. This difference, which can be attributed to the greater permeability of silicone, does not rule out the use of silicone elastomers for seals for environmental containment, air-lock hatch seals, and so forth, for manned spacecraft. The leakage rate measured for silicone, when extrapolated, would amount to only 9.6 cc/day or 3500 cc/year (0.123 cu ft/year). Furthermore, silicone elastomers retain their flexibility to lower temperatures and are more resistant to higher temperatures than the other three elastomers tested.

Figure 16 presents leakage rates as a function of time for the butyl O-ring of figure 15 after 1 and 50 cycles of hatch operation. After 50 cycles of operation the butyl seal performed slightly better than after 1 cycle, but it tended to approach nearly the same equilibrium leakage after $2\frac{1}{2}$ hours.

Figure 17 presents leakage rates as a function of time for a single neoprene O-ring seal after 1 and 50 cycles of operation. Initially the leakage rate after 50 cycles was

somewhat higher than after 1 cycle, but as in the previous test, the leakage rates were approximately the same after $2\frac{1}{2}$ hours. Because even after 3 hours the leakage rate was increasing slightly, the test was continued for 30 hours, at which time leakage had increased to 5.6×10^{-6} cc/sec.

Figure 18 presents leakage rates as a function of time after 1 and 50 cycles for the single viton O-ring.

Figure 19 presents leakage rates as a function of time for the silicone O-ring seal after 1 and 50 cycles. Since permeation through the silicone elastomer is considerably greater than that through the other elastomers tested, a stable leakage rate is achieved in a shorter period of time.

Figure 20 shows a comparison between the leakage measured with a single butyl O-ring in the rectangular groove 2, hatch 1, and the leakage with a butyl O-ring in groove 1, hatch 1. The rectangular groove exposes a larger area of the seal for permeation of the gas, and the seal undergoes a rolling action when the hatch is closed. These two factors may account for the higher leakage.

Hatch 2

A series of tests was made with the seals in groove 1 of hatch 2, which was mounted on the inside of the test chamber so that pressure loading acted to open the hatch.

Figure 21 presents the measured leakage as a function of time for butyl, viton, neoprene, and silicone O-rings. During these tests the leakage rates for neoprene and silicone were lower than in the tests with hatch 1, and the leakage rates for viton and butyl were higher (compare fig. 15). Because the leakage rate for neoprene was unusually low in this test, all instrumentation was checked and recalibrated and the leakage was again measured without disturbing the seal. Almost identical rates were obtained for the second set of measurements. The reason for the unusual performance of neoprene in this case has not been determined.

Figure 22 presents the measured leakage as a function of time for the butyl O-ring after 1 and 50 cycles in groove 1, hatch 2. Considerably greater leakage was measured after 50 cycles, whereas with the O-ring in hatch 1, leakage was slightly greater after 1 cycle than after 50 cycles (fig. 16). This reversal of trends may be caused by decreased seal loading resulting from the pressure loading of the hatch toward the open position, coupled with the undersize cross section of the butyl seal as listed in table I. The nominal cross-section diameter for this size O-ring is 0.275 inch (6.99 mm).

Figure 23 presents the measured leakage as a function of time for the neoprene O-ring in hatch 2 after 1 and 50 cycles of operation. In addition to the reasons listed

for the greater leakage with butyl after 50 cycles, the minimum diameter of the vulcanized joint on the neoprene O-ring, as listed in table I, was undersize.

Figure 24 presents the measured leakage for the viton O-ring in hatch 2 after 1 and 50 cycles of operation. A lower leakage rate was obtained after 50 cycles of operation. The effect of cycling on leakage rates for the viton O-ring was less than that for the butyl and neoprene because of the greater diameter of the viton (table II). This greater diameter would permit the hatch to deflect more before unseating the seal, and initially effect a higher seating stress on the seal.

Figure 25 presents the leakage rate as a function of time for a silicone O-ring seal in hatch 2 after 1 and 50 cycles. A higher leakage rate was measured after 50 cycles. The effects of cycling on the leakage for the silicone O-ring was less than that for butyl and neoprene O-rings because of the larger diameter of the silicone O-ring.

Fixed Joints

Figure 26 presents a plot of measured leakage rate as a function of time after application of helium for joints 1 and 2 with butyl seals. Joint 1 had a maximum leakage rate of 5.6×10^{-6} cc/sec while joint 2 had a maximum leakage rate of 2.3×10^{-6} cc/sec.

Figure 27 presents a plot of leakage rate as a function of time for joint 3 (illustrated in fig. 8). Two butyl O-rings were used in series and the joint was fastened with toggle clamps. Maximum leakage measured in this test was 3.7×10^{-6} cc/sec. The leakage of the two seals in series was not appreciably different from that of the single static seals reported in figure 26.

DISCUSSION

The results of the present investigation have shown that large-diameter hatches of air-lock systems can be sealed reliably. The measurements indicate that O-ring seals made of elastomers could be used for atmospheric containment aboard a manned spacecraft, where leakage of a few cubic centimeters per day would be negligible. Even silicone elastomers, which have a leakage rate almost two orders of magnitude greater than that of the other elastomers tested, would be practical in most cases. Leakage of even a few cubic centimeters per day into systems pumped to high vacuum can be critical, however, since each cubic centimeter expands many orders of magnitude and thus affects the ultimate pressure of the system. Leakage measured in this investigation would not be tolerable in vacuum systems pumped to 10^{-8} torr or less.

The leakage of gases having a higher molecular weight than helium would be much less, since helium will permeate most materials at a higher rate. Air leakage cannot be

measured directly by the system of the present investigation because a single leak cannot be isolated from other leakage sources and from the outgassing products from the inside of the test chamber.

The hatch frames and hatch doors used in this investigation were constructed so that a uniform seating stress could be maintained on the O-ring seal; however, the results of this investigation indicated that a nonuniform seating stress was caused by variations in O-ring cross-sectional diameter. In any air-lock design it is desirable to use the differential pressure loads across the hatch to maintain the seating load on the seals and to prevent inadvertent opening of the hatch; however, this practice is not always compatible with the design of specific configurations. Hatches which have the pressure loads forcing the hatch to the open position require stronger, more complicated latching mechanisms and stiffer hatch frames.

During the present investigation all the seals were used in a clean dry condition except the door shaft seal, which was lubricated with a silicone grease. The application of low-vapor-pressure greases will decrease the leakage rate of seals, but may mask defects in a seal for a period of time. Lubricants may prevent adhesion of the seals to their seating surfaces; however, adhesion did not occur during the 6 months of vacuum testing.

Caution should be observed in using the data reported herein, since the present tests were conducted under laboratory conditions. In actual practice, the seal seating surfaces may become damaged, the seals may be scuffed, cut, or contaminated with foreign material, or the structure may undergo greater deflection from loads, vibration, and uneven temperature distribution.

CONCLUDING REMARKS

Tests of large-diameter O-ring seals have been made on hatches and static joints under laboratory conditions by isolating and measuring leakage of helium through specific areas with a mass spectrometer. Of the four elastomers tested on the operable hatches, butyl, neoprene, viton, and silicone, the silicone had the highest leakage rate (1.41×10^{-4} cc/sec or 12.2 cc/24 hr). Butyl O-rings in static joints had very low leakage rates (less than 6×10^{-6} cc/sec).

The seal leakage values measured were very small when considered from the standpoint of atmospheric containment aboard a manned spacecraft. Even the helium leakage of the silicone O-ring would be almost negligible for this use.

Repeated opening and sealing of the hatch had less effect on leakage rates when the hatch was forced against the seating flange by pressure than when it was being forced open by pressure.

Additional research is needed to define the leakage of other types of molded and inflatable elastomeric seals and to determine the effects of temperature extremes and vibration on leakage of seals.

Langley Research Center,
National Aeronautics and Space Administration,
Langley Station, Hampton, Va., October 31, 1967,
124-08-01-04-23.

REFERENCES

1. Trout, Otto F., Jr.: Sealing Manned Spacecraft. Astronaut. Aerospace Eng., vol, 1, no. 7, Aug. 1963, pp. 44-46.

2. Anon.: Space Station Connection and Seal Study. Contract NAS1-2164, Environmental Res. Associates (Randallstown, Md.), Oct. 1962.

3. Mauri, R. E.: Seals and Gaskets. Space Materials Handbook, Claus G. Goetzel and John B. Singletary, eds., Contract AF 04(647)-673, Lockheed Missiles and Space Co., Jan. 1962, pp. 325-348.

4. Farkass, Imre; and Barry, Edward J.: Study of Sealants for Space Environment. NRC Res. Proj. No. 43-1-139 (Contract DA-19-020-506-ORD-5097), Nat. Res. Corp. (Cambridge, Mass.), 1960.

5. Everett, Malcolm H.; and Gillette, Howard G.: Molded Packings: Squeeze-Type. Machine Design, vol. 36, no. 14, June 11, 1964, pp. 59-66.

TABLE I.- VARIATIONS IN O-RING SIZE

Material	Cross-section diameter of extruded stock		Minimum diameter at vulcanized joints
	Minimum	Maximum	
Butyl	0.261 inch (6.63 mm)	0.275 inch (6.99 mm)	0.267 inch (6.78 mm)
Neoprene	0.268 inch (6.81 mm)	0.278 inch (7.06 mm)	0.253 inch (6.43 mm)
Viton	0.277 inch (7.04 mm)	0.302 inch (7.67 mm)	0.270 inch (6.86 mm)
Silicone	0.270 inch (6.86 mm)	0.304 inch (7.72 mm)	0.270 inch (6.86 mm)

TABLE II.- SUMMARY OF TEST DATA

Test	Location and composition of seals	Maximum measured leakage of helium, cc/sec (STP)	Leakage of helium based on 24 hr, cc/day (STP)
	Entire exposed end of air lock		
1	Grooves 1, 2, and 3 and static joints; butyl	4.01×10^{-5}	3.5
2	Grooves 1, 2, and 3 and static joints; butyl	4.2×10^{-5}	3.6
3	Grooves 1, 2, and 3 and static joints; butyl	5.2×10^{-5}	4.5
	Hatch 1		
4	Groove 1; butyl	1.05×10^{-6}	0.09
5	Groove 1; butyl (after 50 cycles)	8.0×10^{-7}	.07
6	Groove 1; neoprene	4.3×10^{-6}	.37
7	Groove 1; neoprene (after 50 cycles)	4.4×10^{-6}	.38
8	Groove 1; viton	2.8×10^{-6}	.24
9	Groove 1; viton (after 50 cycles)	1.9×10^{-6}	.16
10	Groove 1; silicone	1.12×10^{-4}	9.7
11	Groove 1; silicone (after 50 cycles)	1.41×10^{-4}	12.2
12	Groove 2; butyl	1.01×10^{-4}	8.7
	Hatch 2		
13	Groove 1; butyl	7.9×10^{-6}	0.68
14	Groove 1; butyl (after 50 cycles)	1.03×10^{-4}	8.9
15	Groove 1; neoprene	1.4×10^{-7}	.12
16	Groove 1; neoprene (after 50 cycles)	6.3×10^{-5}	5.4
17	Groove 1; viton	6.3×10^{-6}	.54
18	Groove 1; viton (after 50 cycles)	1.21×10^{-6}	.105
19	Groove 1; silicone	3.4×10^{-5}	2.9
20	Groove 1; silicone (after 50 cycles)	6.3×10^{-5}	5.4
	Static joints		
21	Joint 1; butyl	5.6×10^{-6}	0.48
22	Joint 2; butyl	2.3×10^{-6}	.20
23	Joint 3; butyl	3.7×10^{-6}	.32

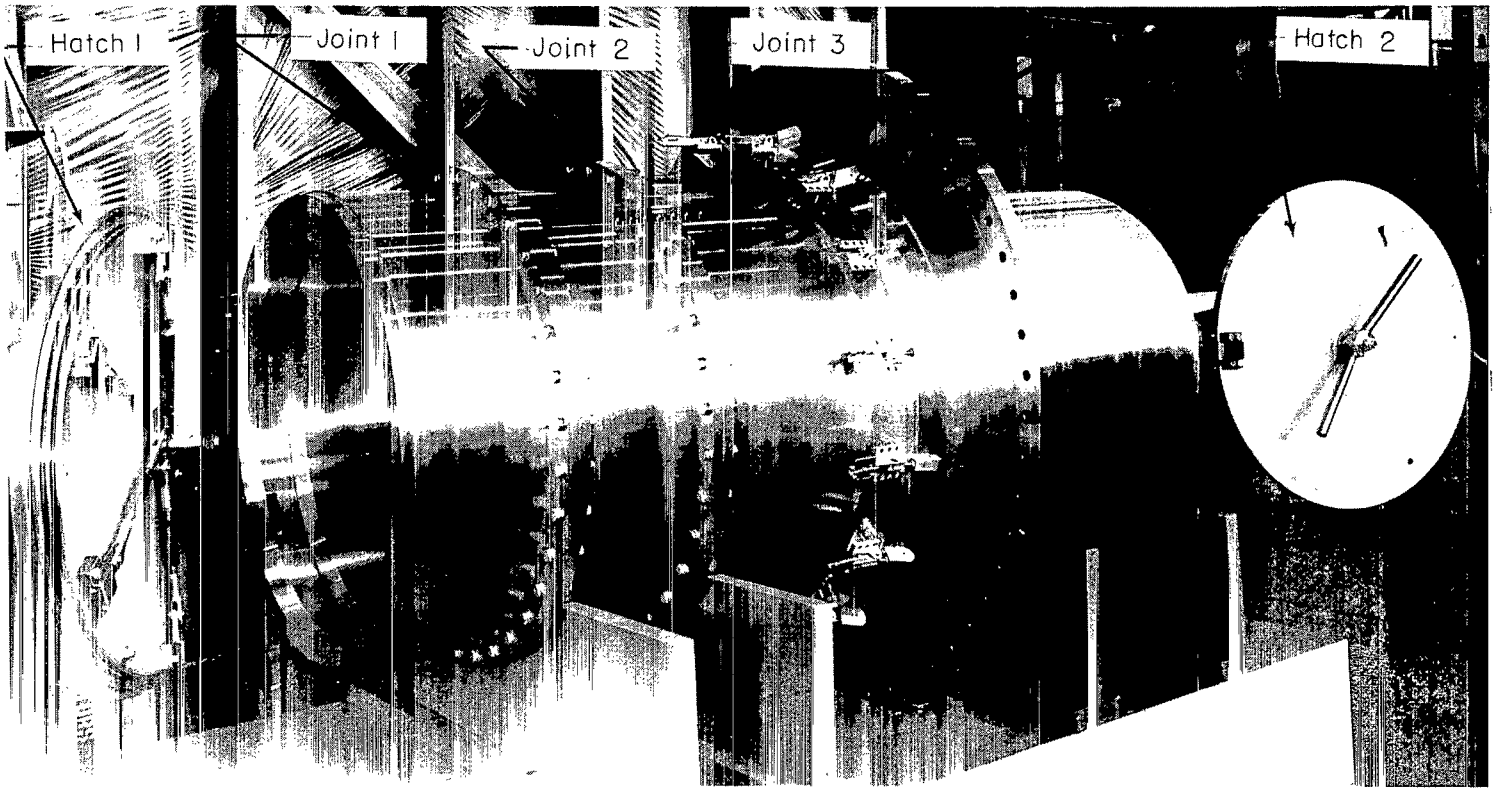

Figure 1.- Air-lock test model.

L-64-1324.1

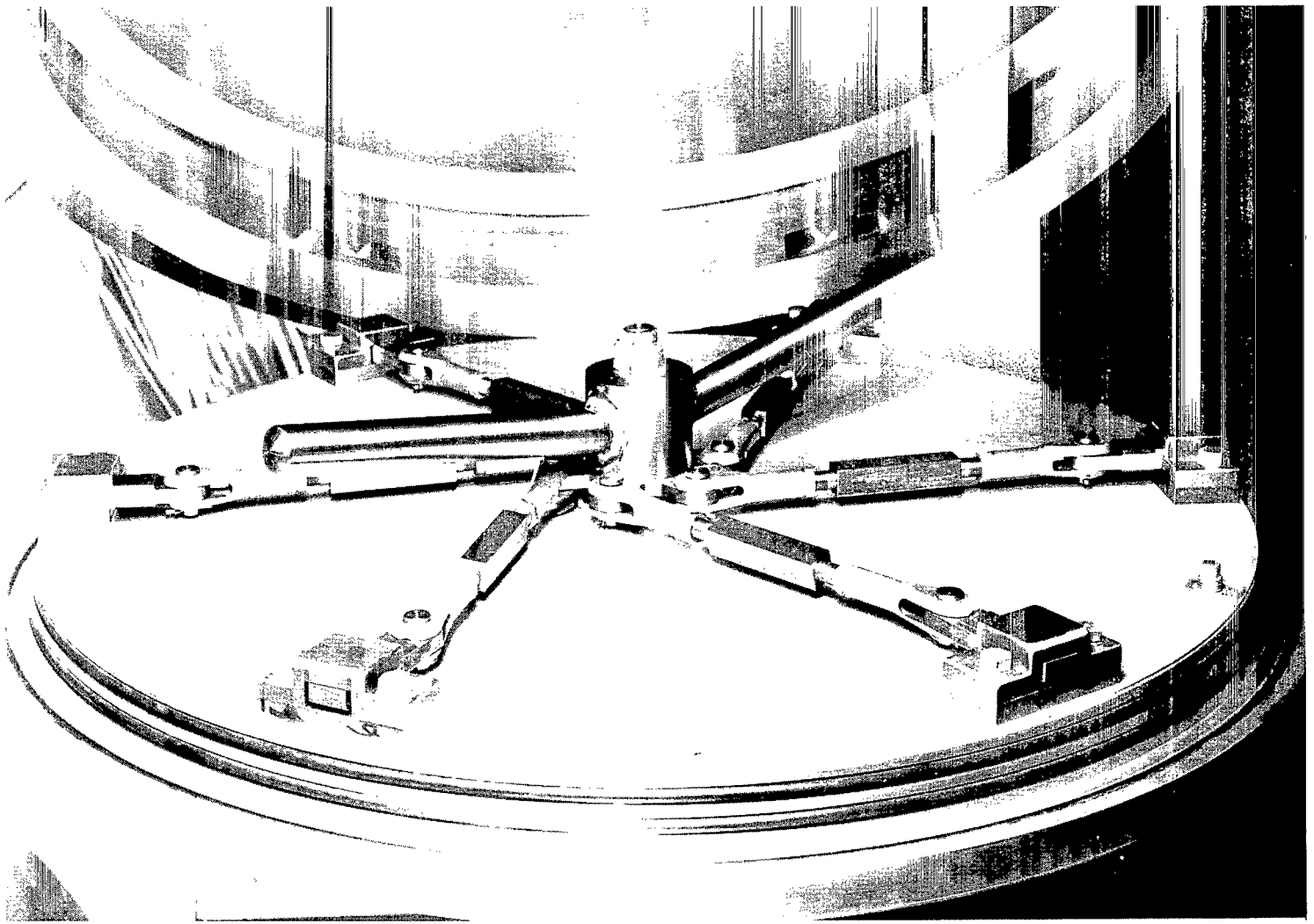

Figure 2.- The hatch door with the cam-actuated latch mechanism and the O-ring seals. L-64-1325

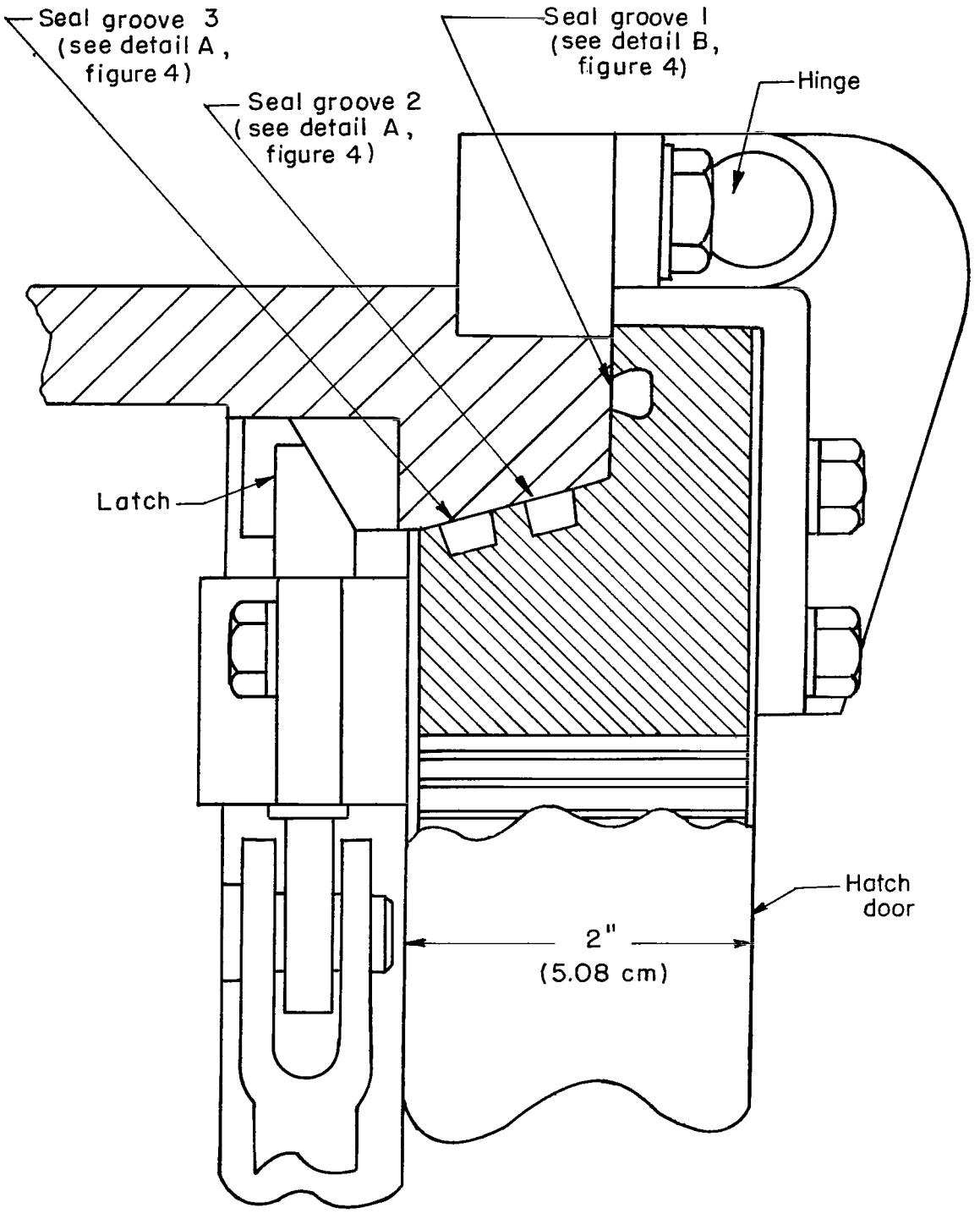

Figure 3.- Cross section of the hatch door seated in the hatch frame.

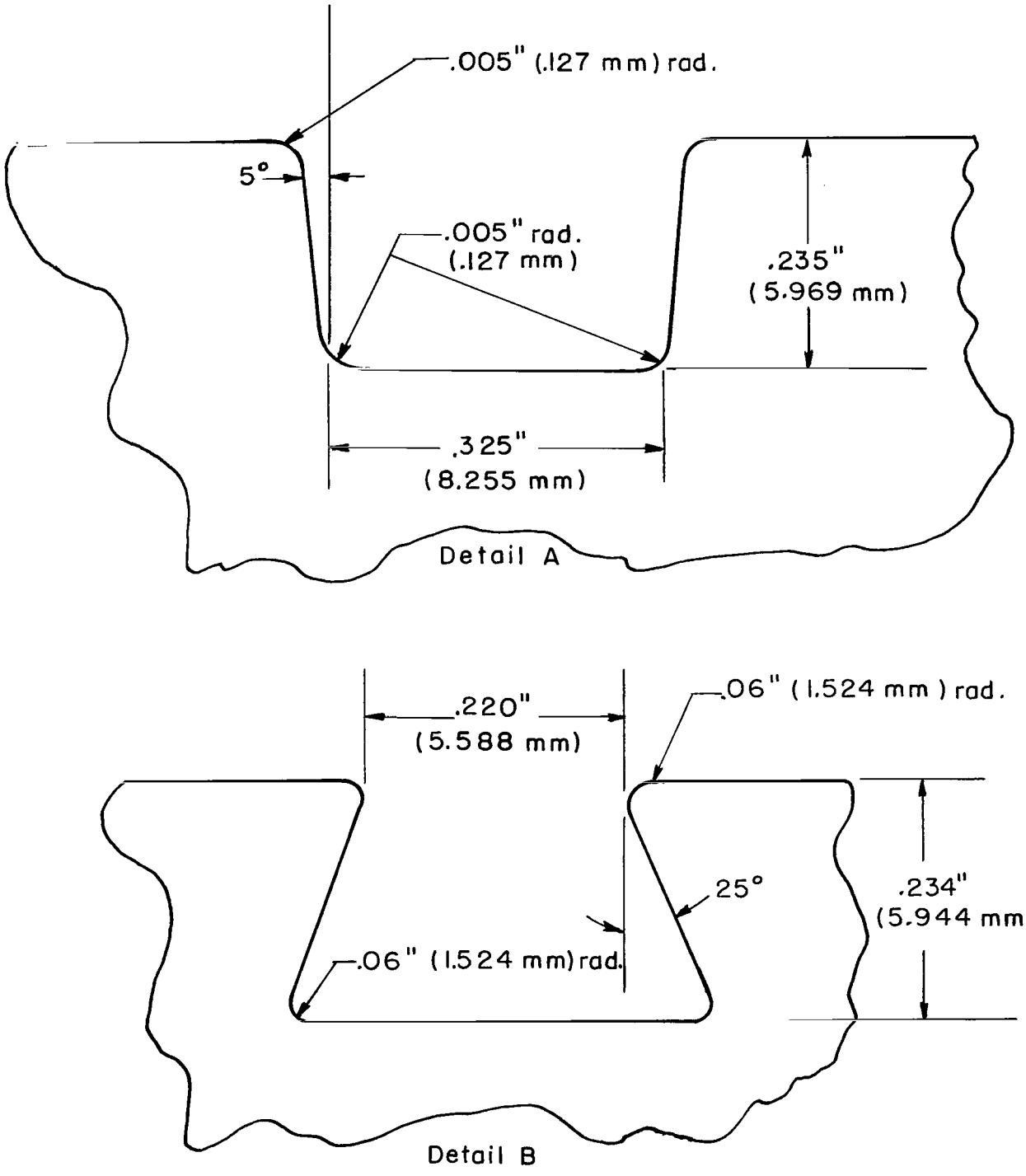

Figure 4.- Cross section of the O-ring seal grooves.

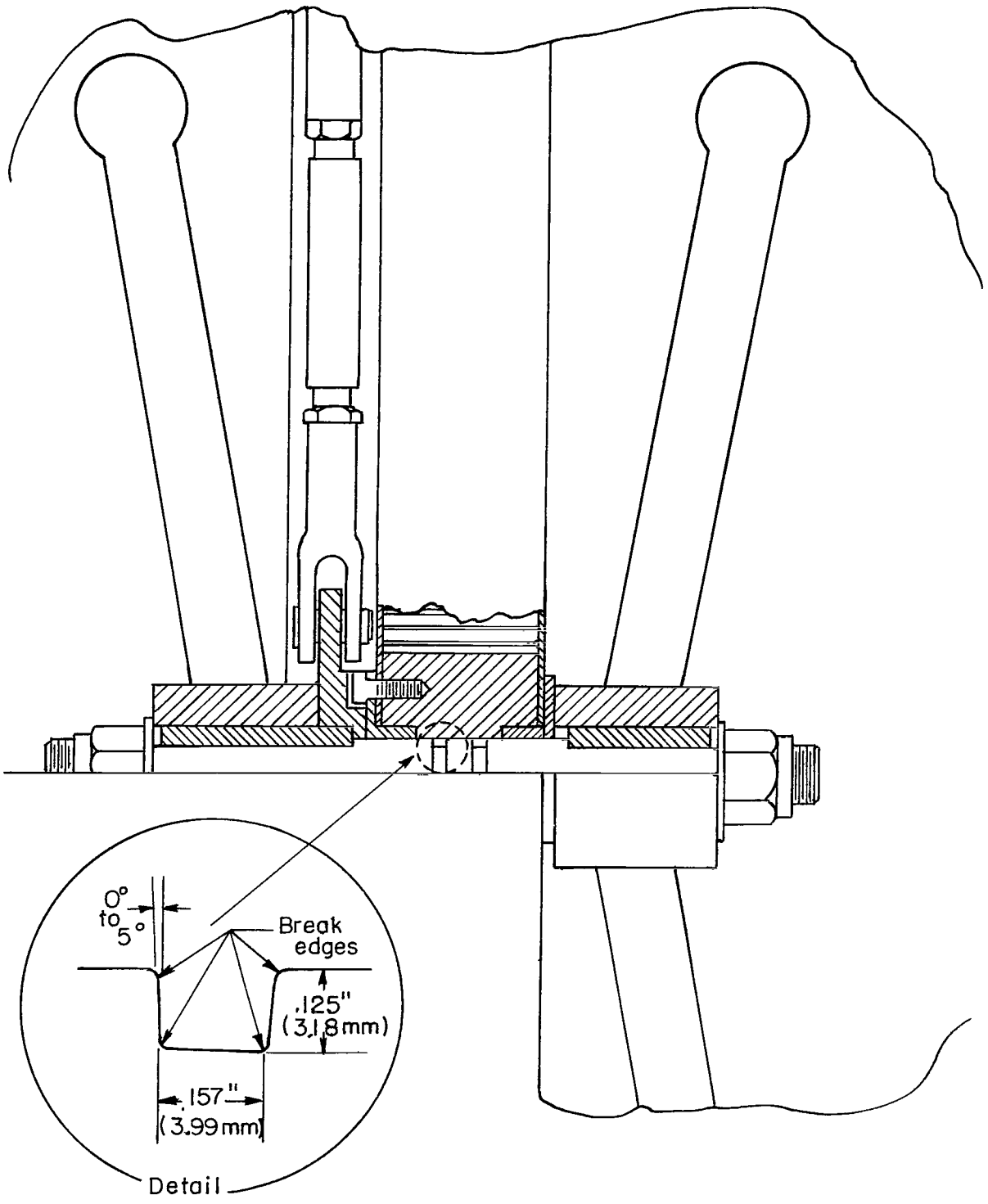

Figure 5.- Cross section of the center shaft of the hatch door.

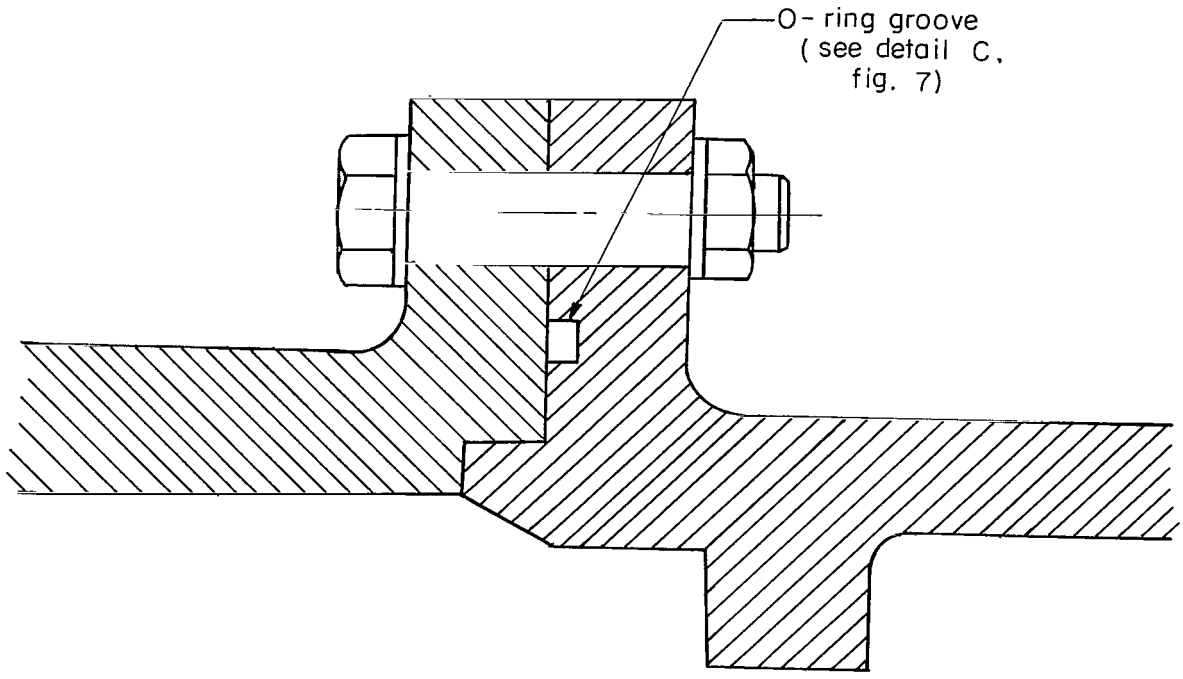

Figure 6.- Cross section of static joints 1 and 2.

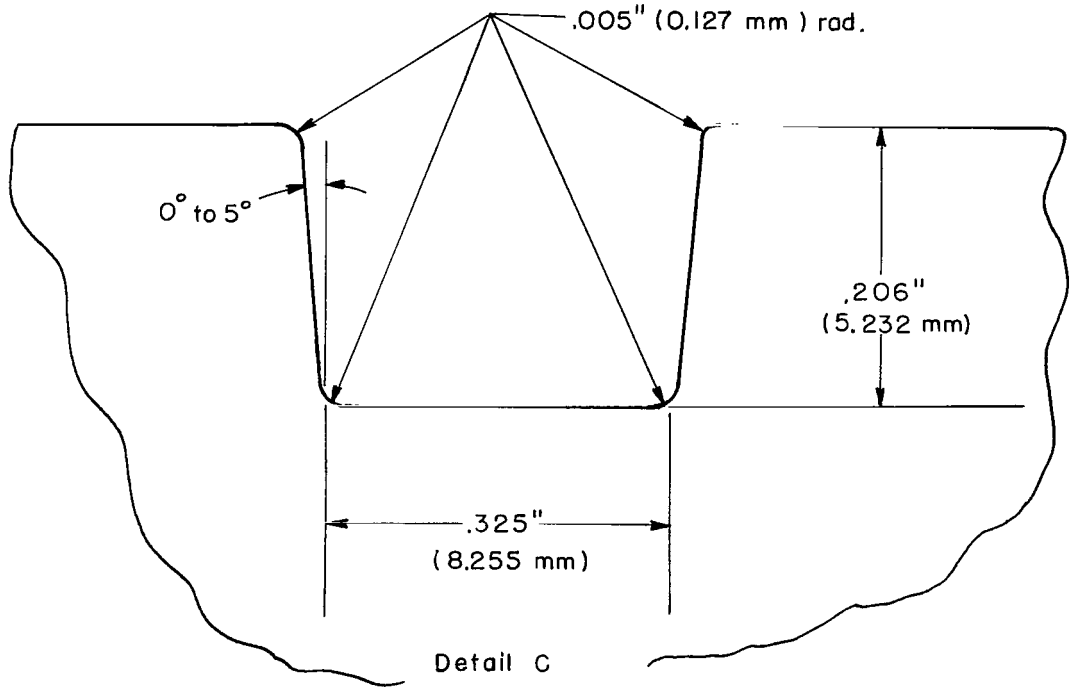

Figure 7.- Cross section of the O-ring grooves used in joints 1 and 2.

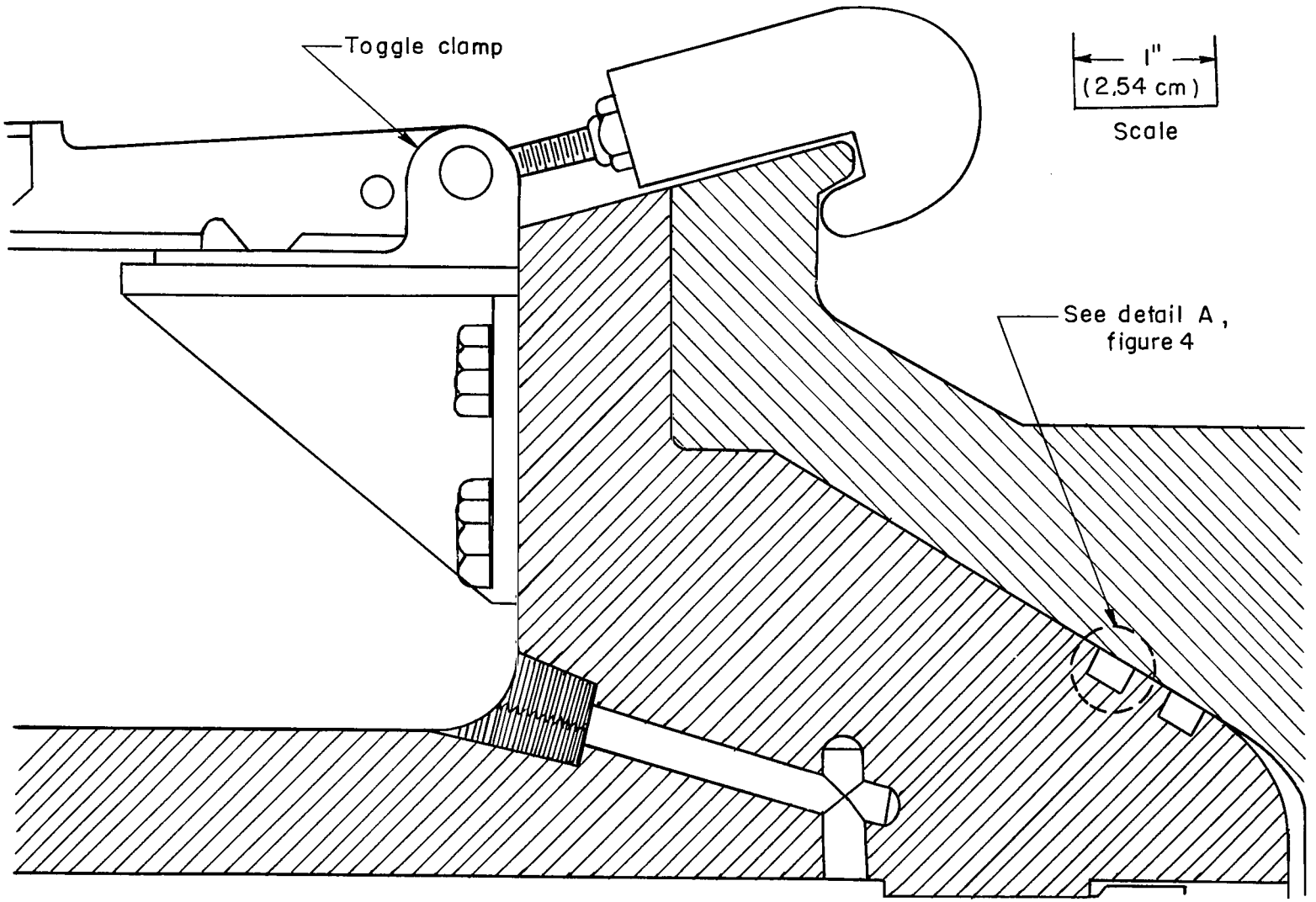

Figure 8.- Cross section of joint 3.

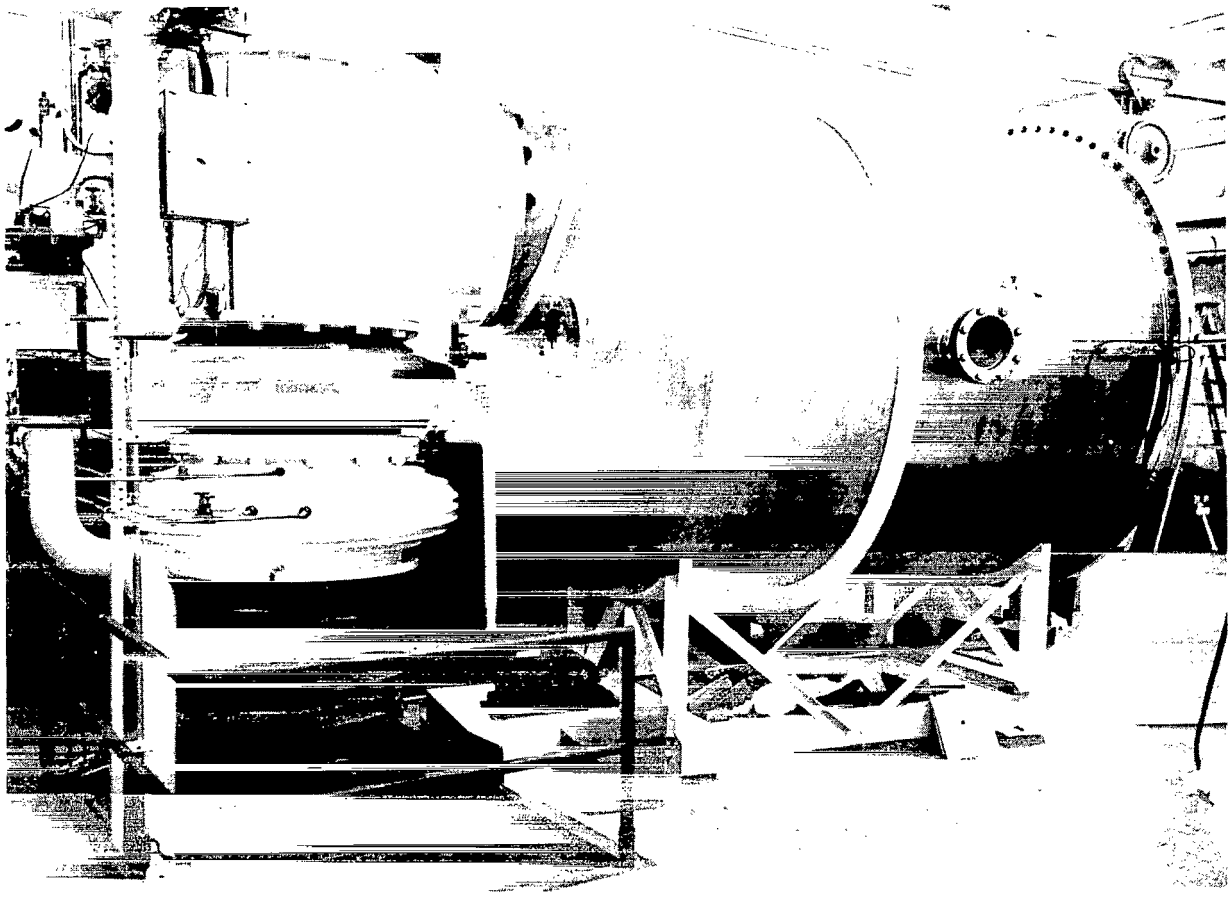

Figure 9.- Vacuum test chamber. L-64-844

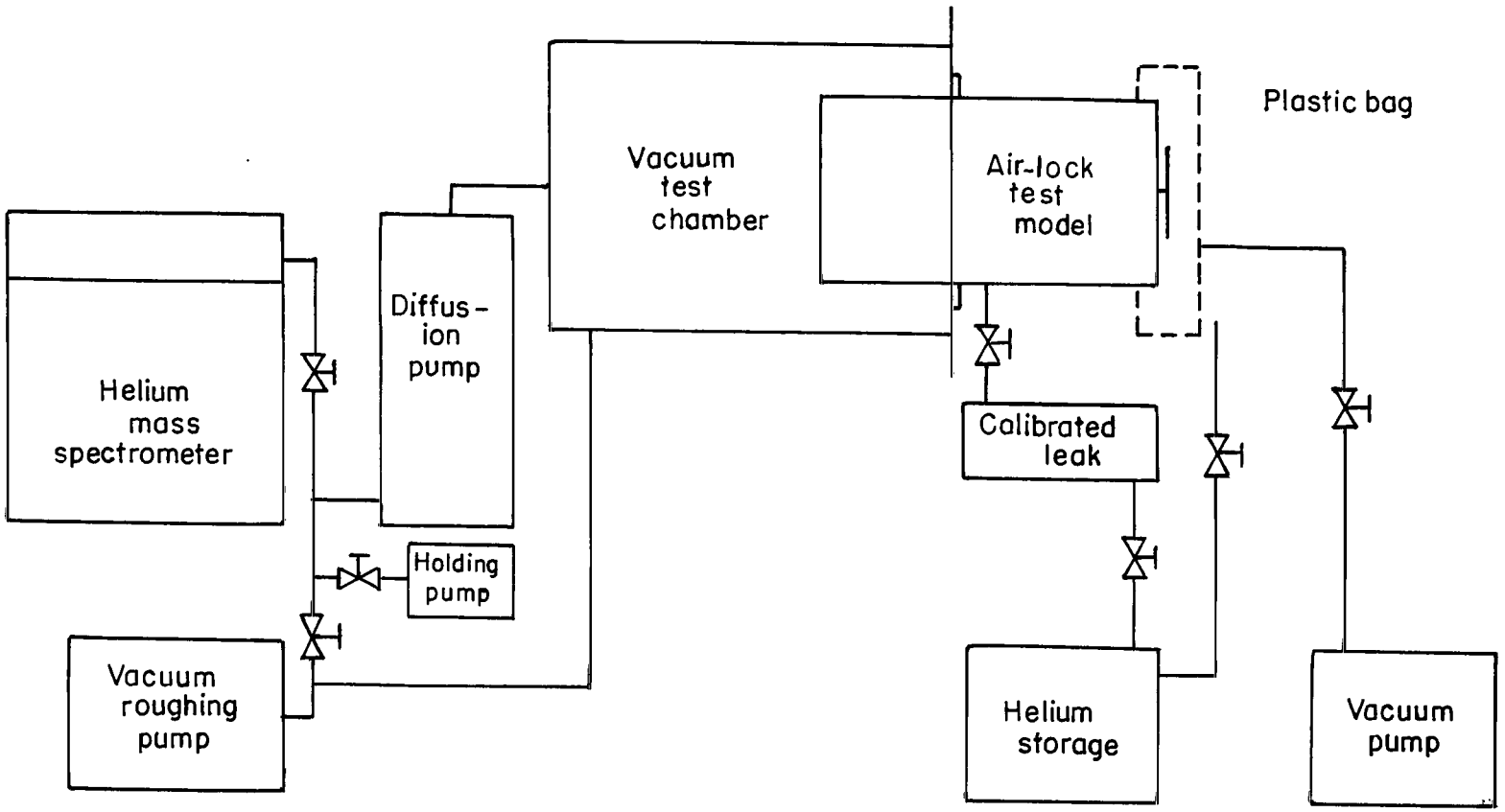

Figure 10.- Diagram of the leak measuring system.

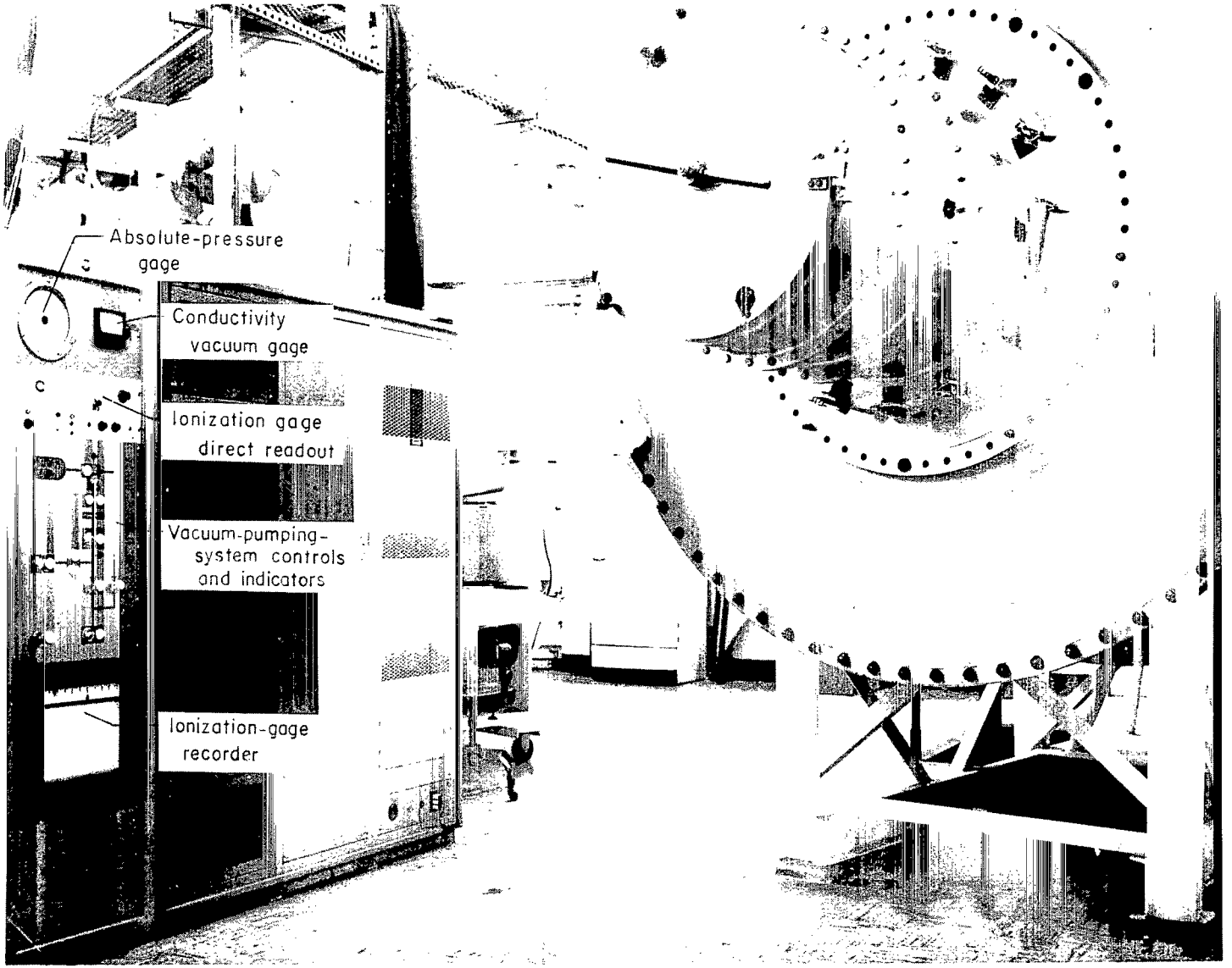

Figure 11.- Instrument panel for the vacuum test chamber.

L-64-3959.1

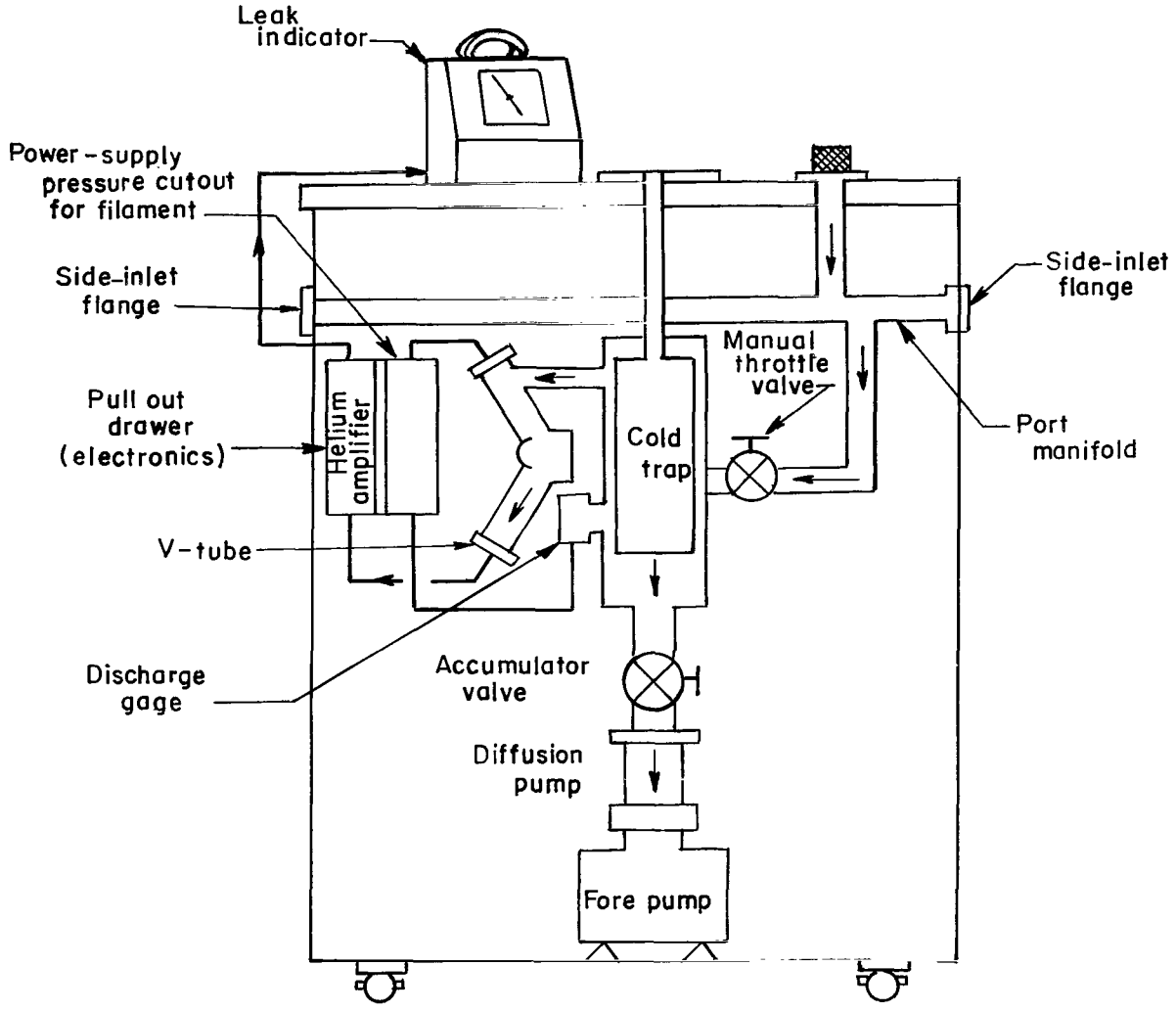

Figure 12.- Helium mass-spectrometer leak detector.

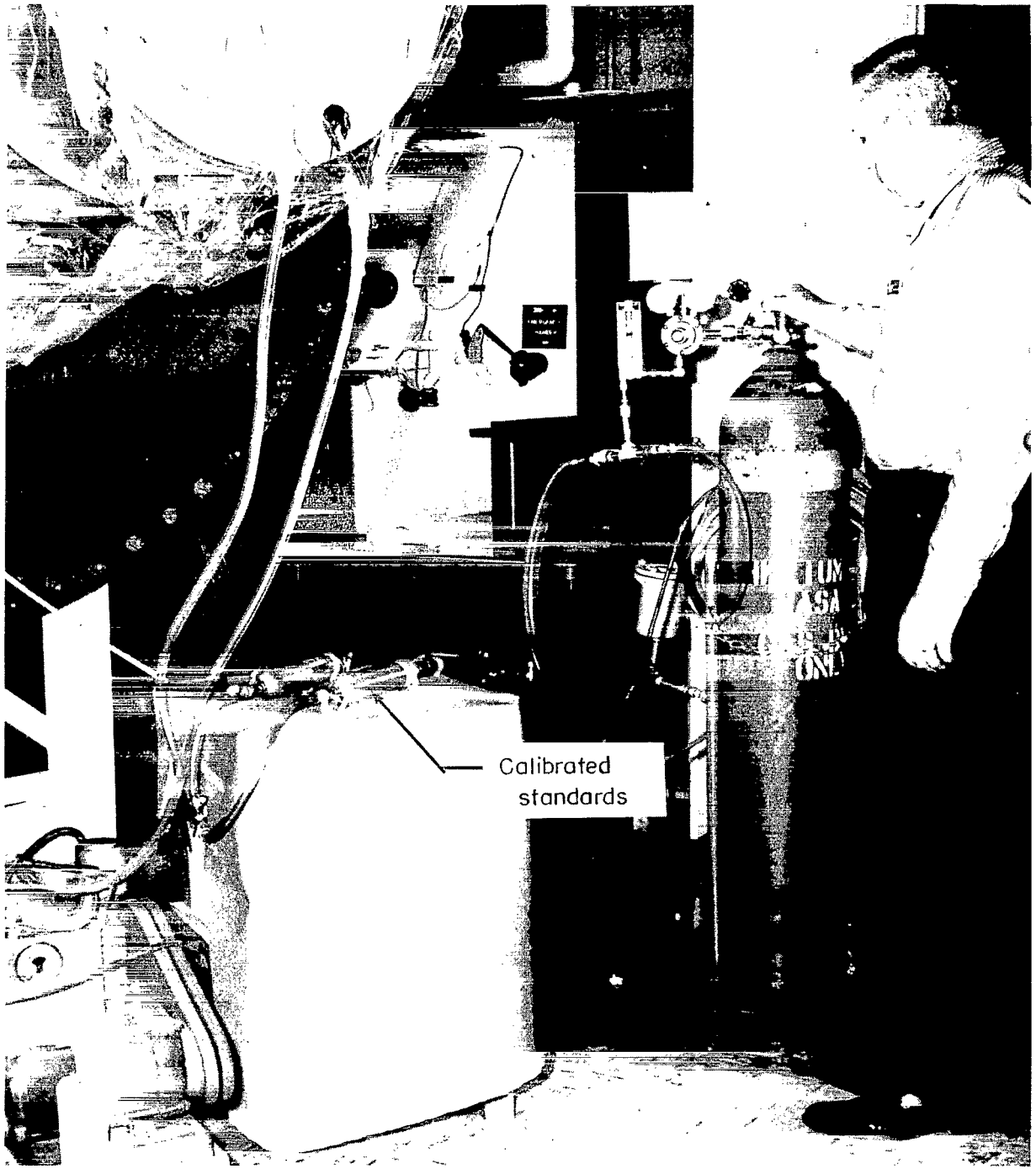

Figure 13.- Photograph of the encapsulated air lock and the calibrated leak standards. L-64-11543.1

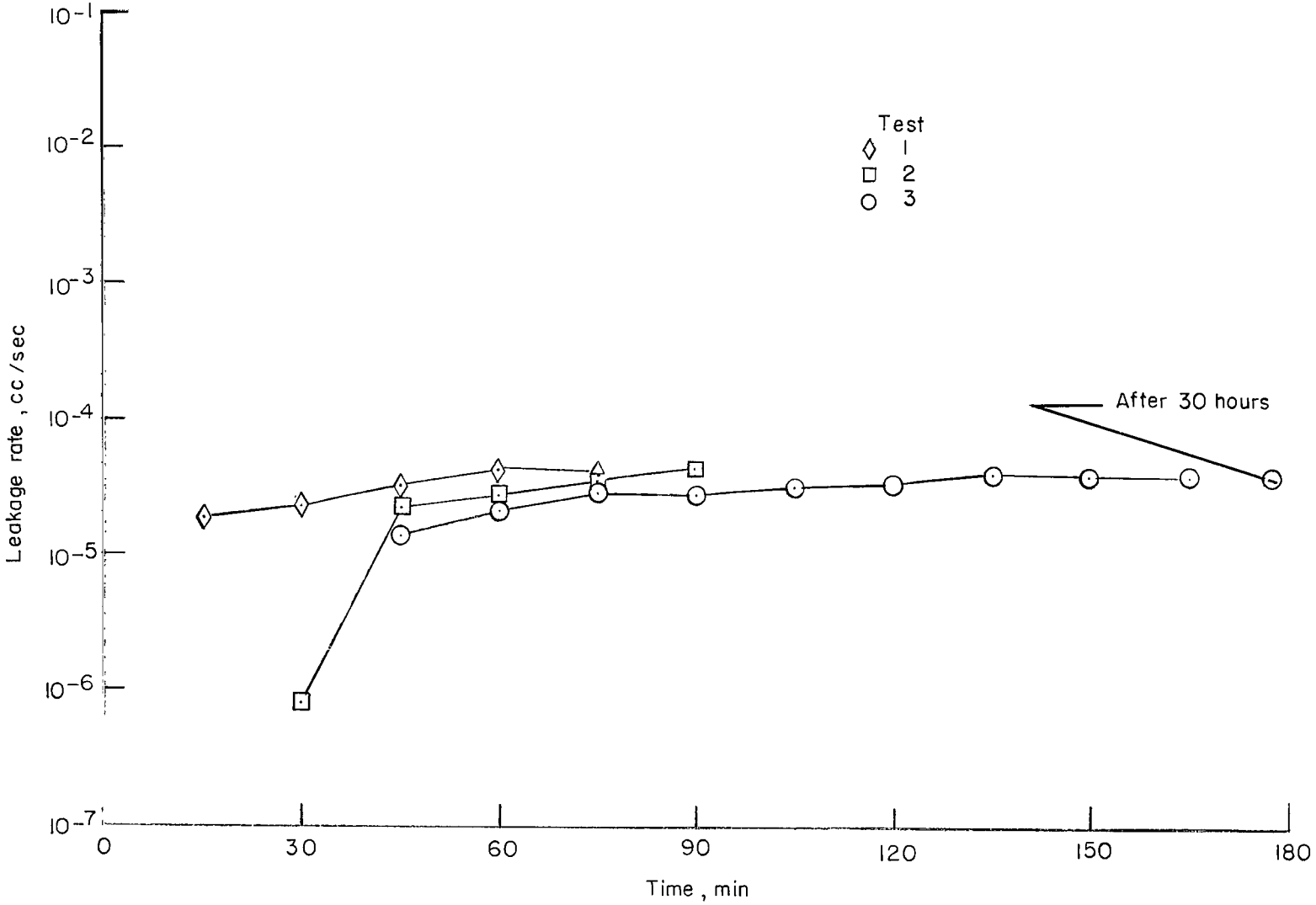

Figure 14.- Leakage rate as a function of time for the exposed end of the air lock with butyl O-ring seals in all three grooves and the static joints of hatch 1.

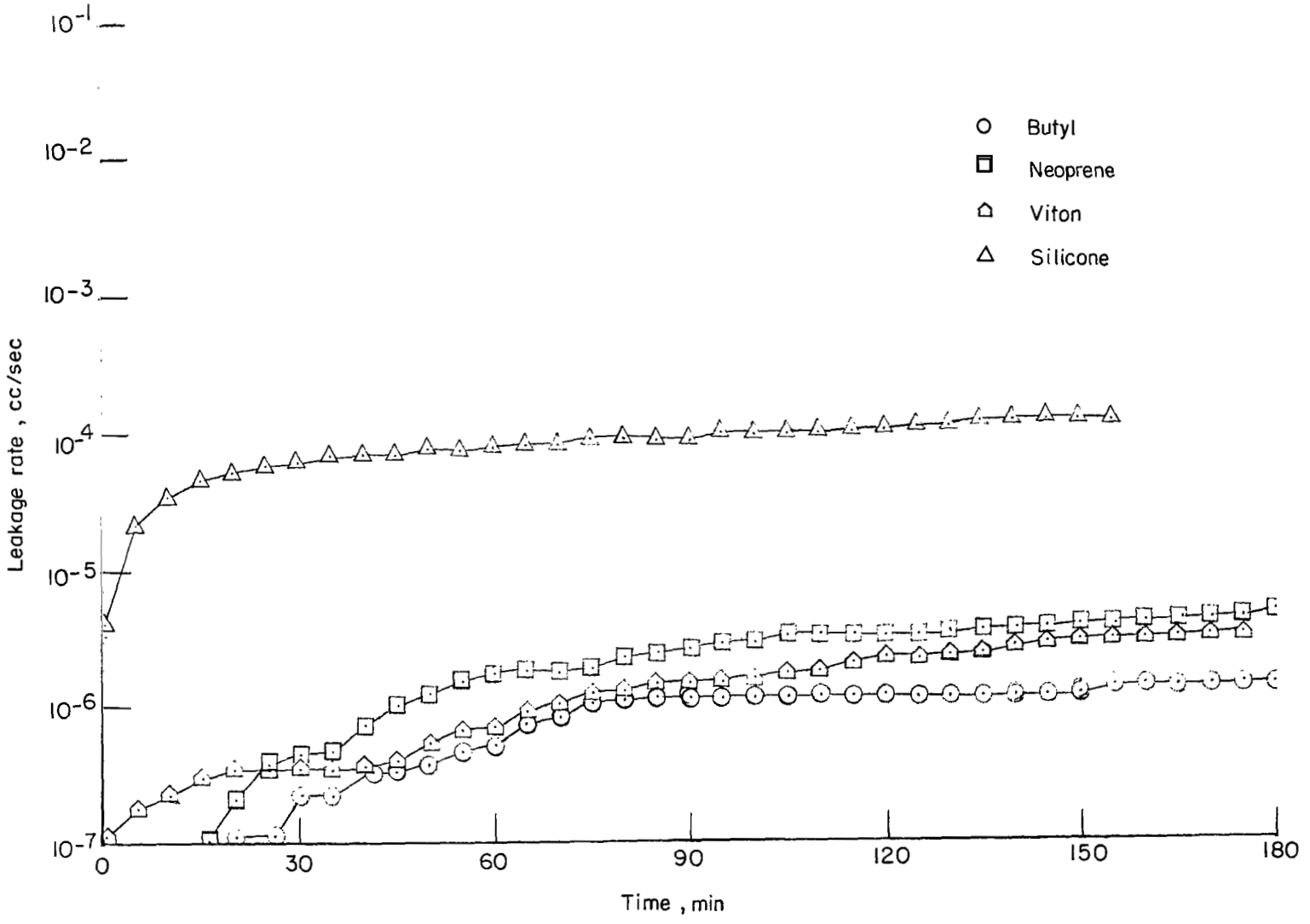

Figure 15.- Leakage rate as a function of time for butyl, neoprene, viton, and silicon O-ring seals in groove 1 of hatch 1.

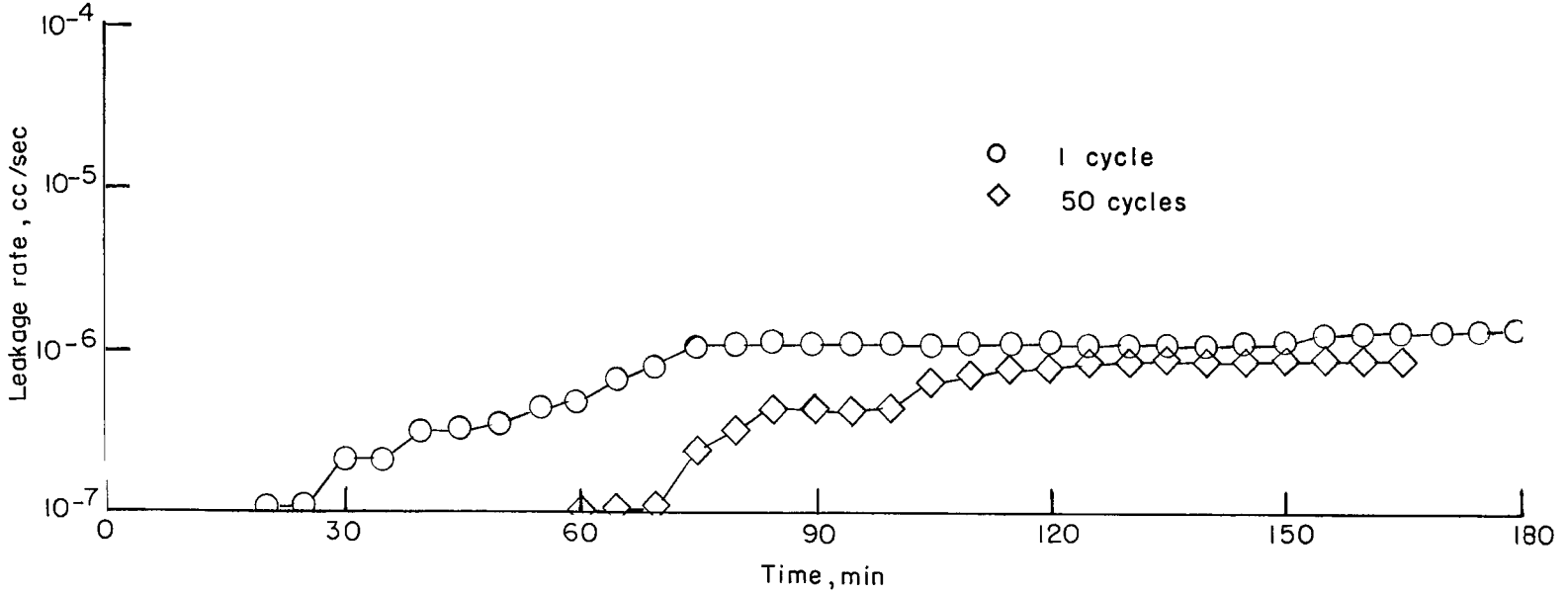

Figure 16.- Leakage rate as a function of time for butyl O-ring seal in groove 1 of hatch 1.

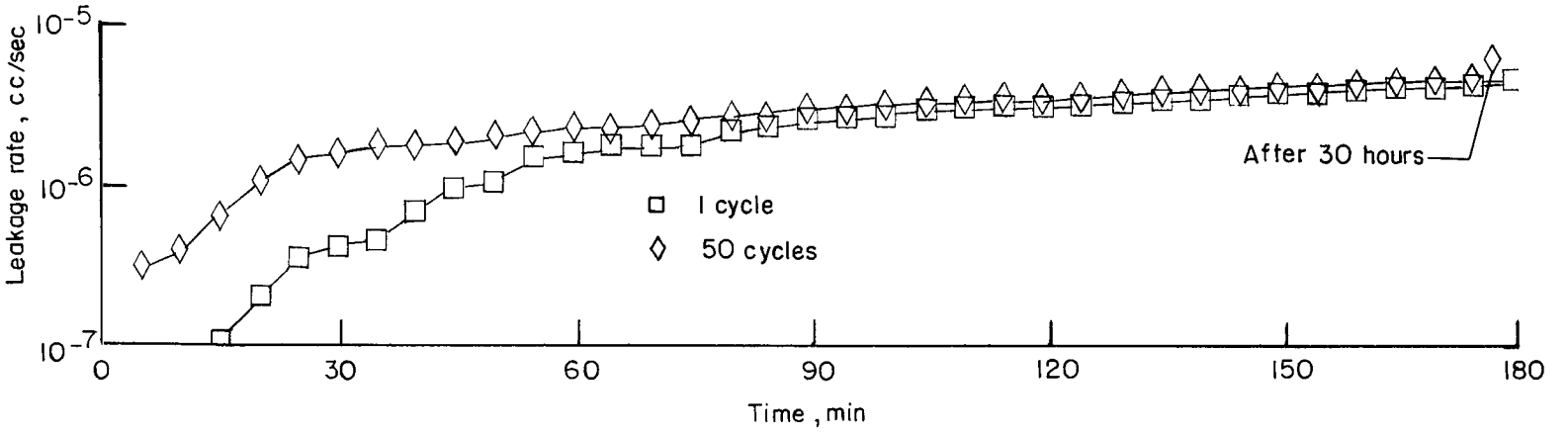

Figure 17.- Leakage rate as a function of time for neoprene O-ring seal in groove 1 of hatch 1.

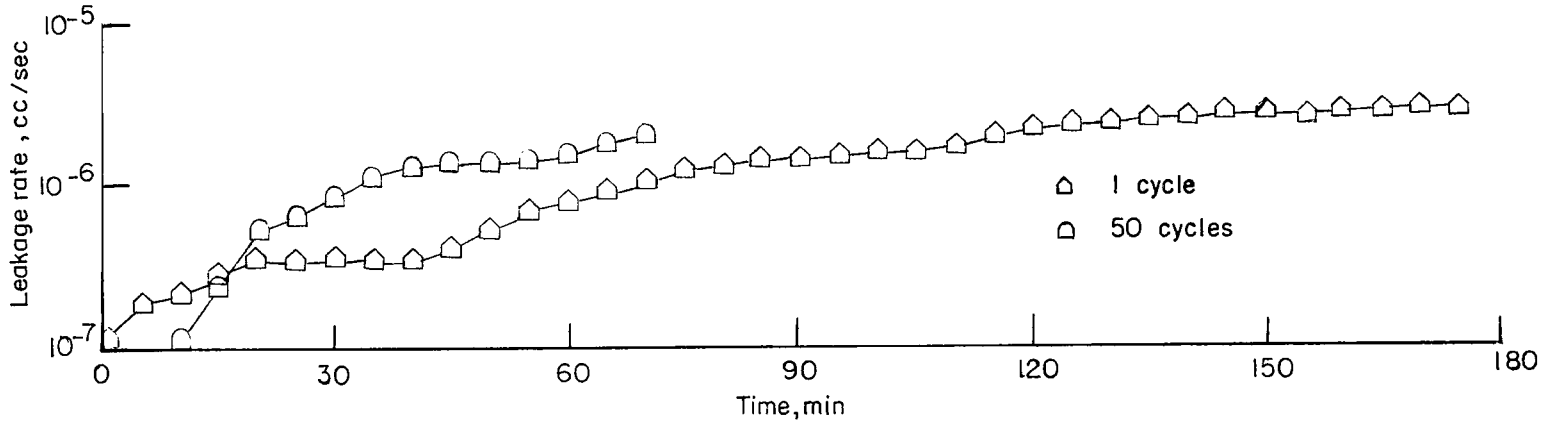

Figure 18.- Leakage rate as a function of time for viton O-ring seal in groove 1 of hatch 1.

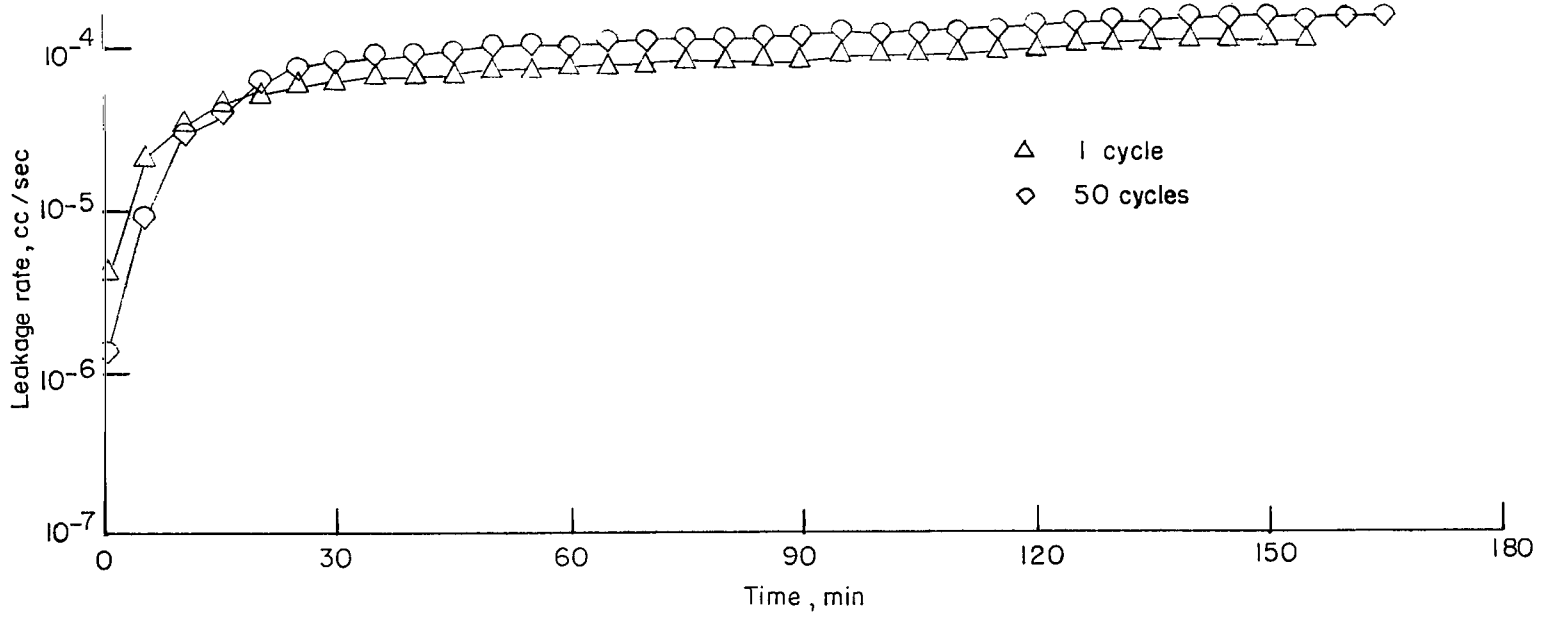

Figure 19.- Leakage rate as a function of time for silicone O-ring seal in groove 1 of hatch 1.

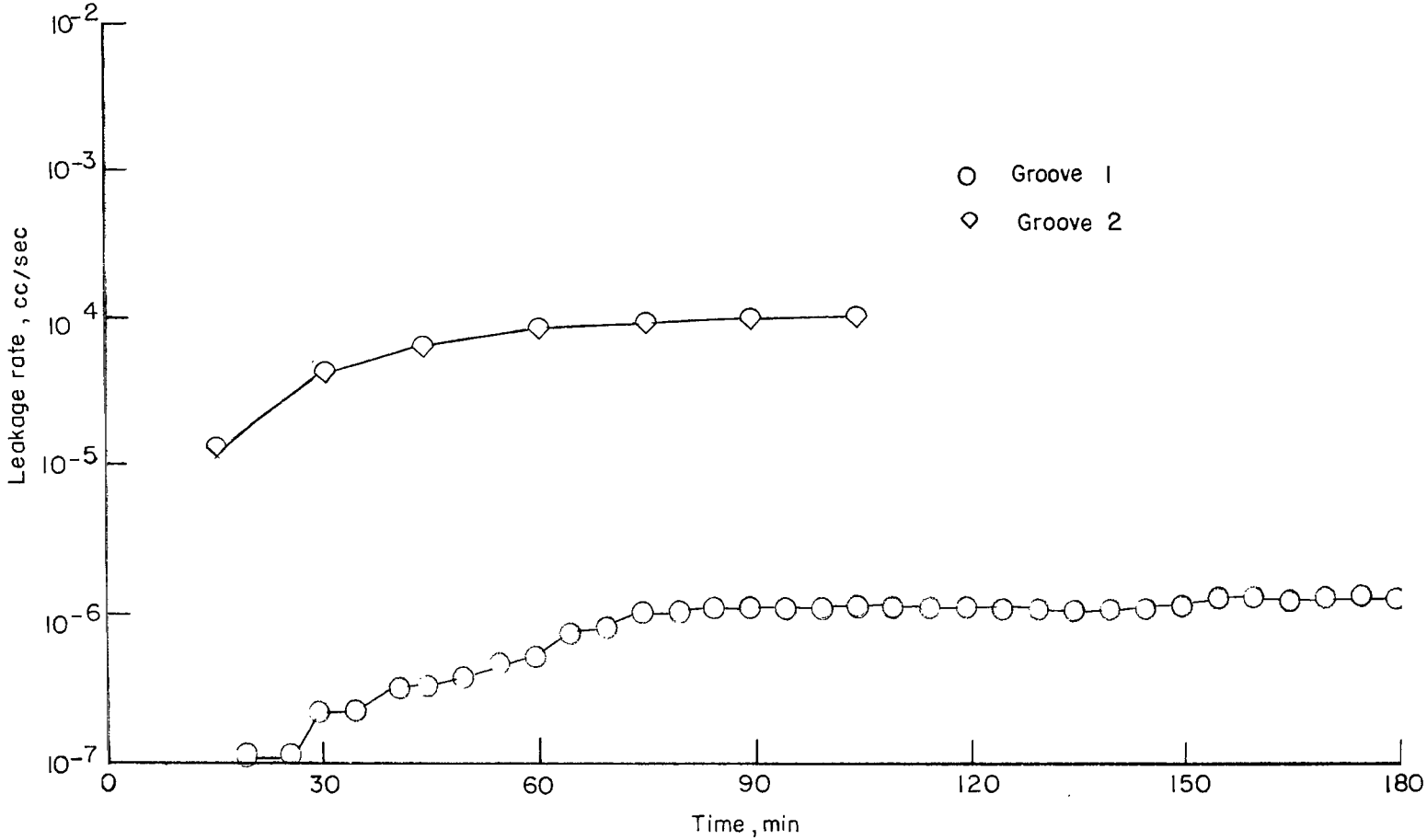

Figure 20.- Leakage rate as a function of time for butyl O-ring seals in groove 1 of hatch 1 and groove 2 of hatch 1.

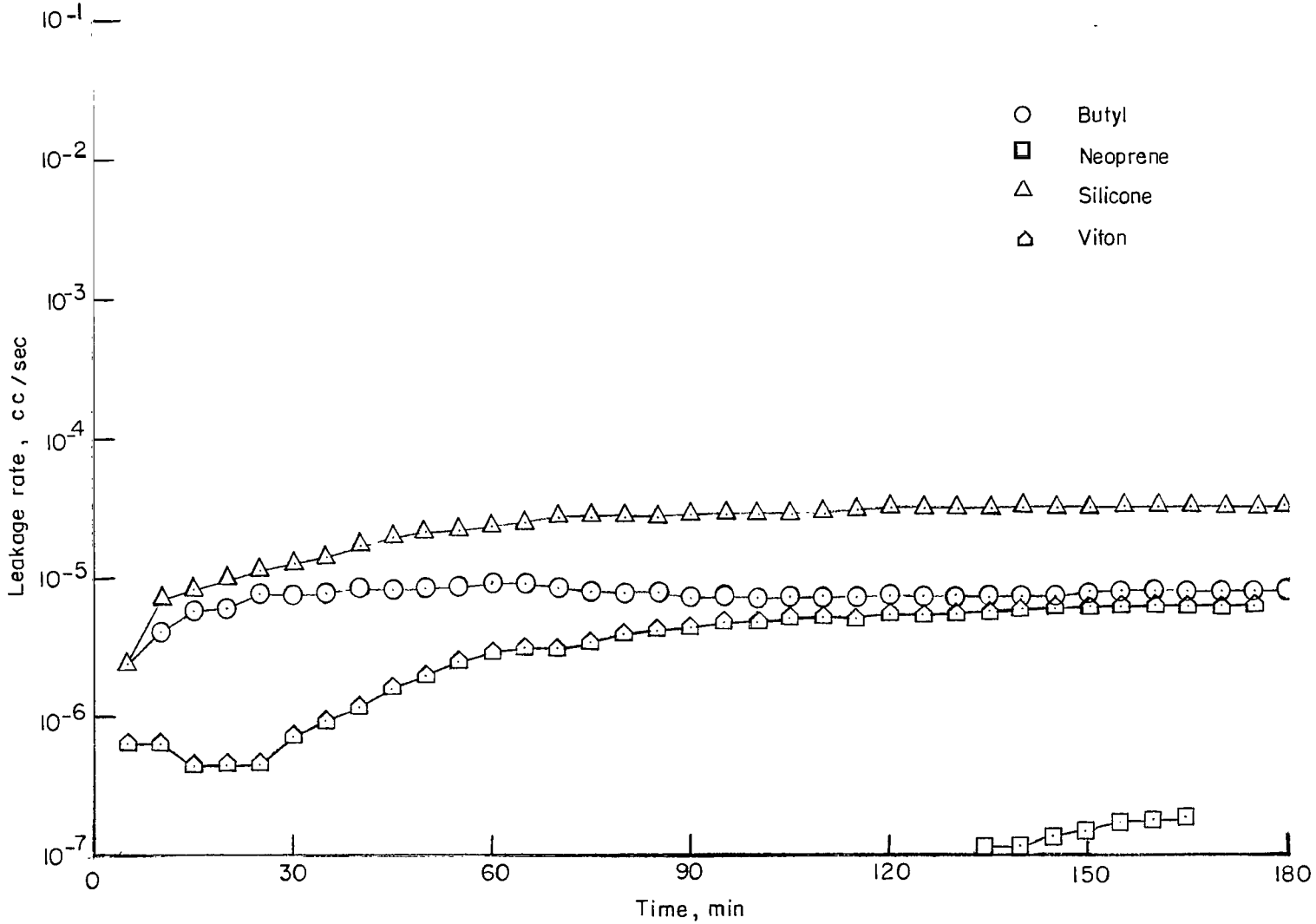

Figure 21.- Leakage rate as a function of time for butyl, neoprene, viton, and silicon O-ring seals in groove 1 of hatch 2.

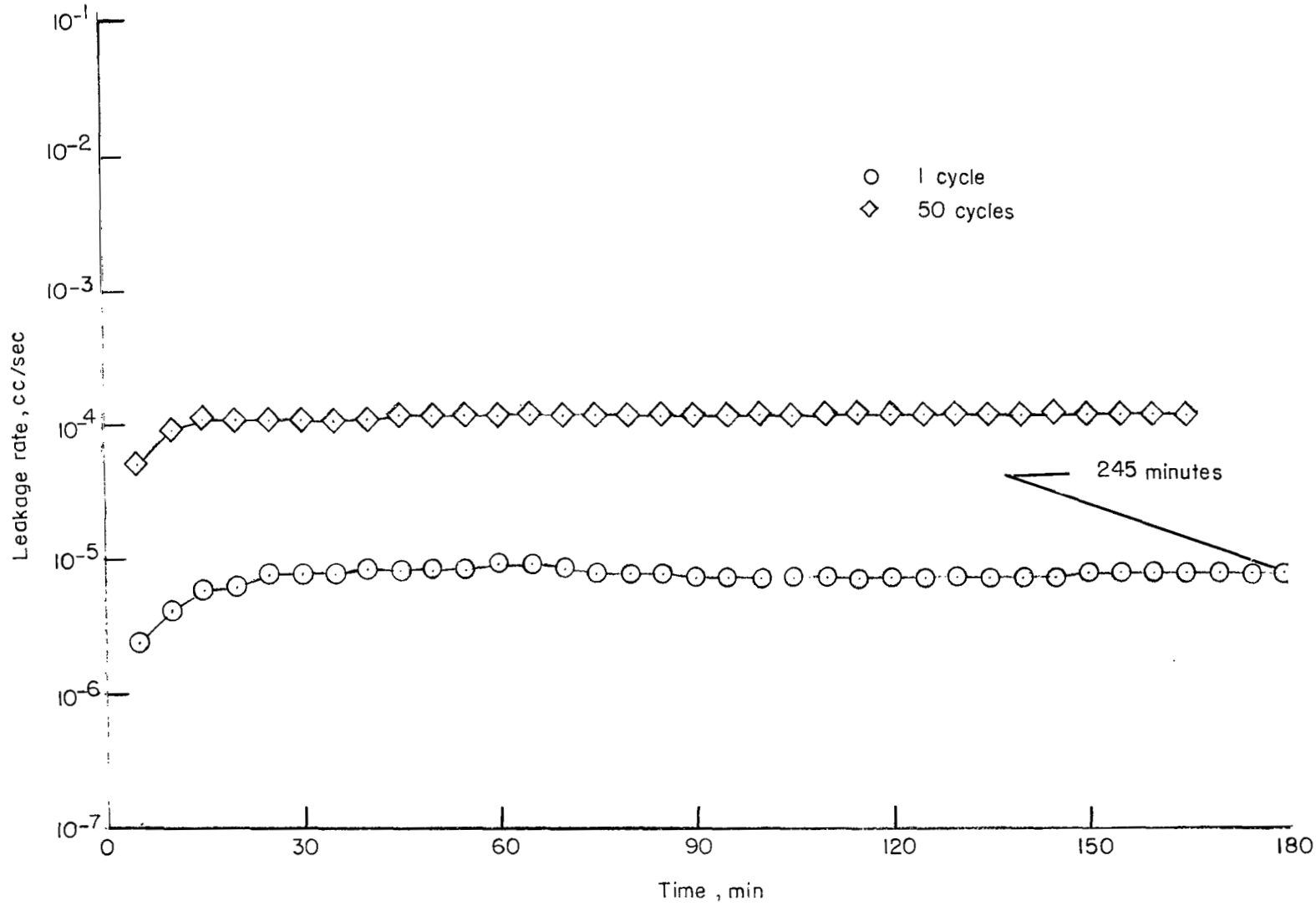

Figure 22.- Leakage rate as a function of time for butyl O-ring seal in groove 1 of hatch 2.

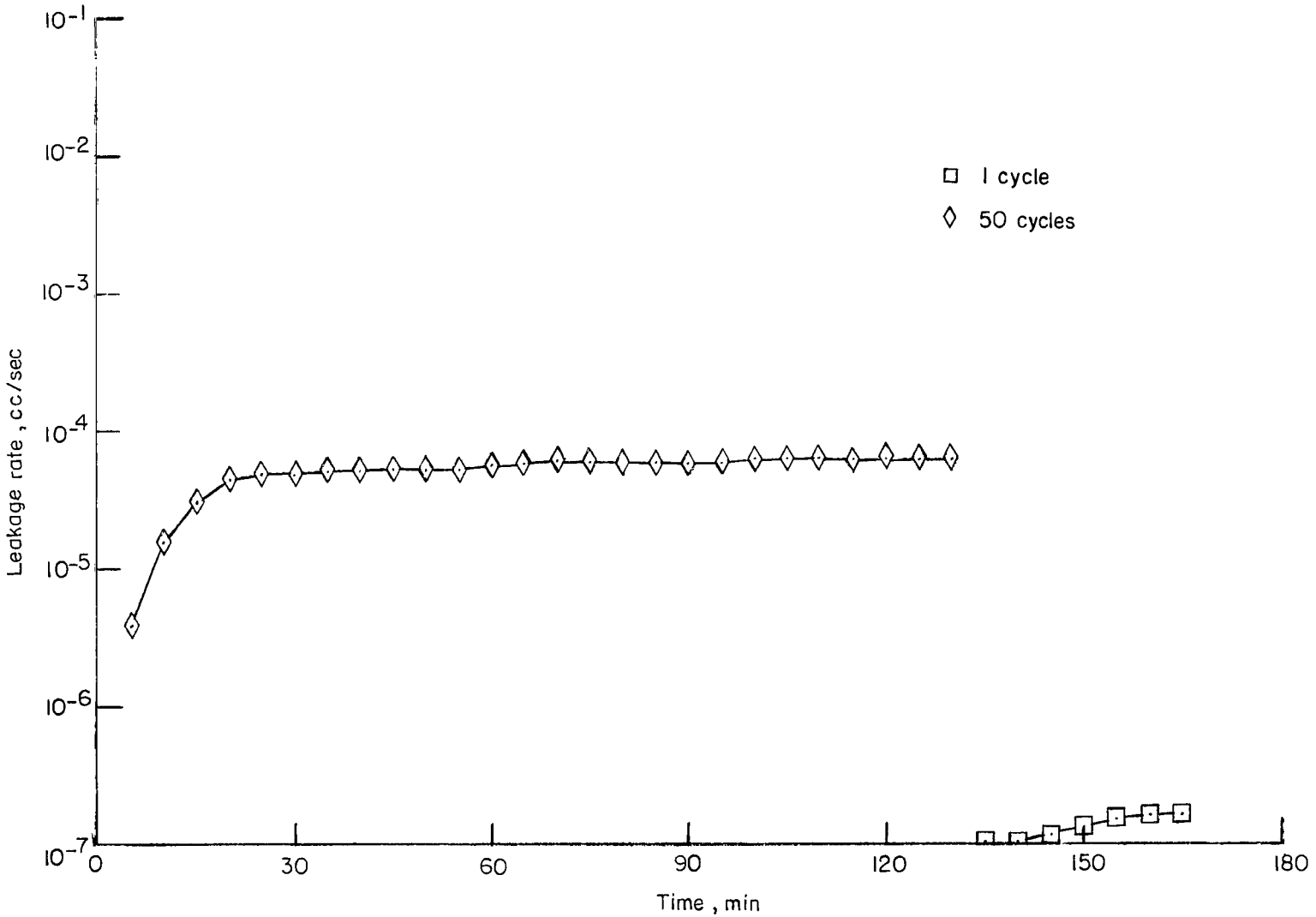

Figure 23.- Leakage rate as a function of time for neoprene O-ring seal in groove 1 of hatch 2.

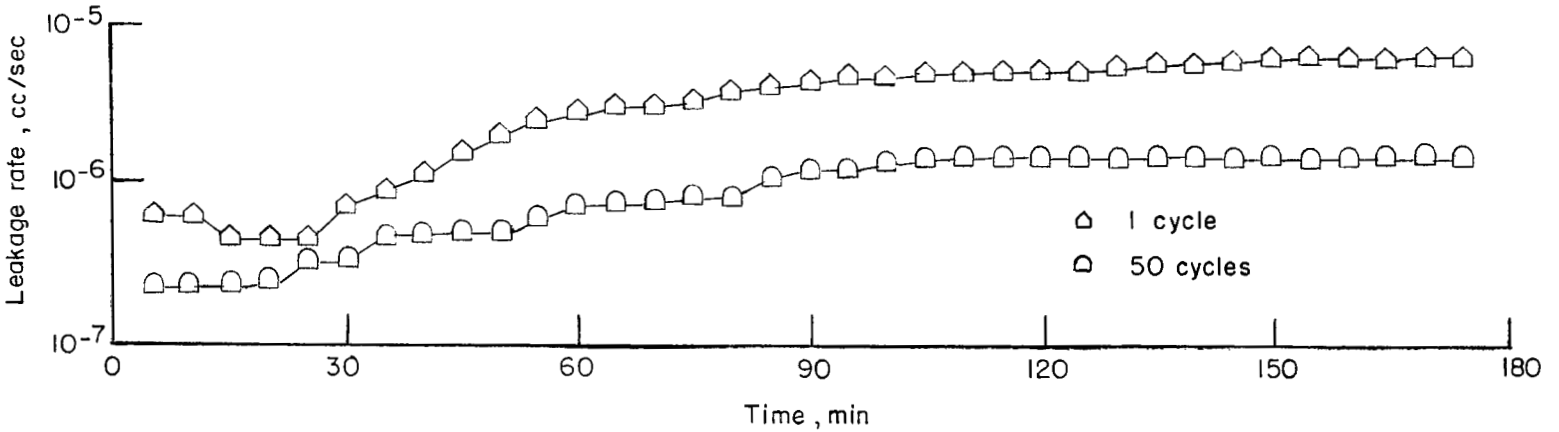

Figure 24.- Leakage rate as a function of time for viton O-ring seal in groove 1 of hatch 2.

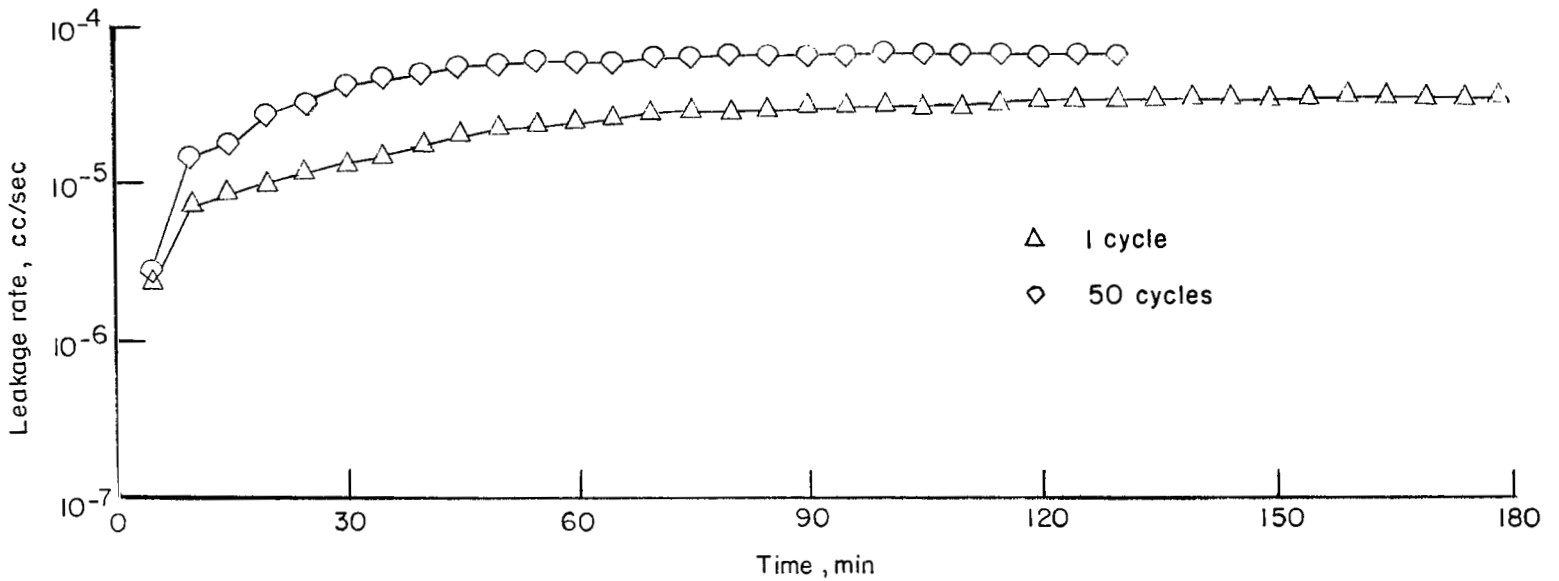

Figure 25.- Leakage rate as a function of time for silicone O-ring seal in groove 1 of hatch 2.

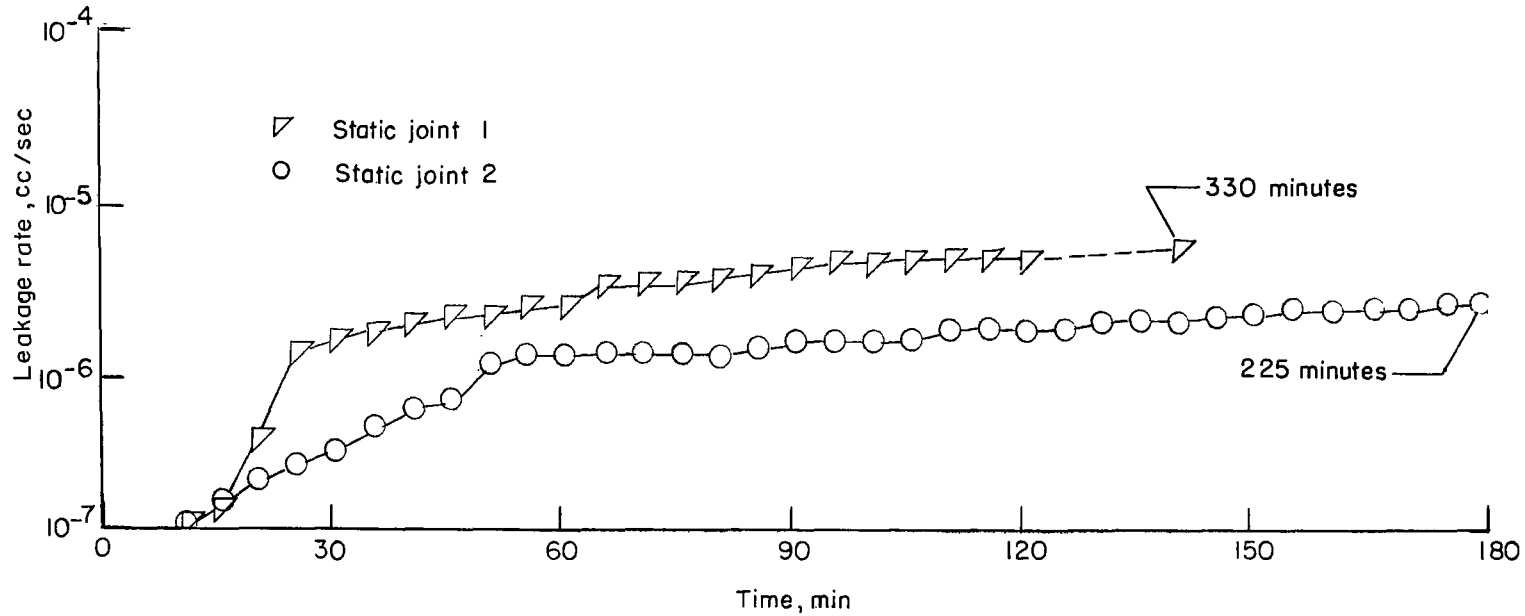

Figure 26.- Leakage rate as a function of time for butyl O-ring seals in static joints 1 and 2.

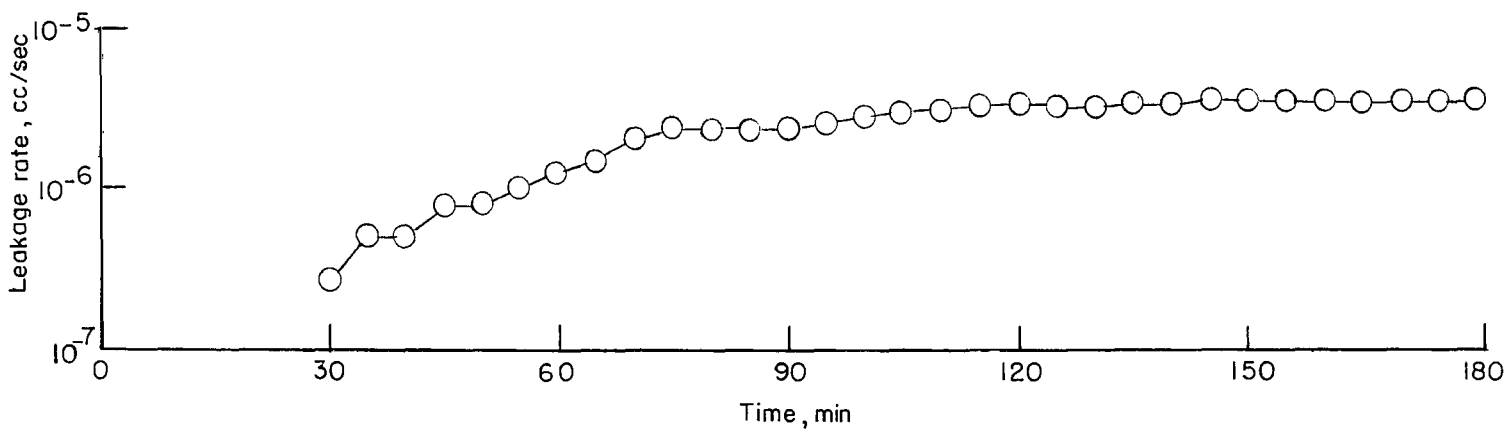

Figure 27.- Leakage rake as a function of time for butyl O-ring seal in static joint 3.